UNIVERSITAT POLITÈCNICA DE VALÈNCIA

Escola Tècnica Superior d'Enginyeria Agronòmica i del Medi Natural

UNIVERSITAT POLITÈCNICA DE VALÈNCIA

School of Agricultural Engineering and Environment

THE ROLE OF THE TRANSCRIPTION FACTOR ZINC FINGER PROTEIN 423 (ZNF423) IN THE DIFFERENTIATION OF INSULIN RECEPTOR SUBSTRATE 2 (IRS2) SILENCED ADIPOCYTES

End of Degree Project

Bachelor's Degree in Biotechnology

AUTHOR: López Padilla, Lorena

Tutor: Bueso Ródenas, Eduardo

External cotutor: NAVARRO GONZALEZ, MARIA DEL CARMEN

Experimental director: CAROBBIO, STEFANIA

ACADEMIC YEAR: 2022/2023

THE ROLE OF THE TRANSCRIPTION FACTOR ZINC FINGER PROTEIN 423 (ZNF423) IN THE DIFFERENTIATION OF INSULIN RECEPTOR SUBSTRATE 2 (IRS2) SILENCED ADIPOCYTES

End of degree project

Bachelor's degree in Biotechnology

Academic year 2022/2023

Universitat Politècnica de València - ETSEAMN

Author: Lorena López Padilla

Experimental Director: Dr. Stefania Carobbio

External cotutor: María del Carmen Navarro González

Academic tutor: Eduardo Bueso Ródenas

Valencia, July 2023

ABSTRACT

Obesity is a multifactorial disease that originates from a combination and interaction of genetic and environmental factors. It is associated with an increased susceptibility to suffer other pathologies such as diabetes, cardiovascular diseases or development of different types of cancer. Obesity is determined by an imbalance of energy intake vs utilisation. The excess of energy is stored as fat in adipocytes, which are the main adipose tissue's constituent cells. Adipocytes come from a multipotent subset of mesenchymal stem cells that undergo a process called adipogenesis by which they become mature fat cells.

Insulin receptor substrate 2 (IRS2) is involved in adipogenesis, being part of the insulin signalling pathway. It has been demonstrated that adipocyte precursors in IRS2 knockout (KO) mice show an impairment in the differentiation into mature adipocytes.

Previous works have described the zinc finger protein 423 (ZNF423) transcription factor as a key factor in white and brown adipocytes commitment and differentiation. Preliminary data suggest that ZNF423 could have a role downstream IRS2 in the insulin signalling pathway.

The objective of this work was to study if ZNF423 could play a role in IRS2 KO adipocytes differentiation process, which could lead to the identification of a possible target to rescue their differentiation capabilities. To do that, different experiments were carried out.

At first, ZNF423 levels were measured by RT-qPCR in IRS2 KO and control mice in fed and fasted states. In addition, to understand the behaviour of IRS2 and ZNF423 during adipocyte differentiation, 3T3-L1 mouse preadipocytes were infected with lentiviruses carrying constructs for IRS2 overexpression and silencing. The mRNA and protein levels of ZNF423 and other genes of interest were measured by RT-qPCR and western blot, respectively. In addition, morphological analysis of adipocytes was performed by immunofluorescence.

The morphological analysis showed that the adipocytes underwent the typical morphological changes expected during adipocyte differentiation. The results of the mouse experiments show that the mRNA expression levels of IRS2 and ZNF423 seem to follow the same pattern. Furthermore, the same could be observed in the silencing experiment in 3T3-L1 cells. This could indicate that ZNF423 is located downstream of IRS2 in the insulin signalling cascade.

KEY WORDS: IRS2, ZNF423, adipocyte differentiation, adipose tissue, obesity, lipids, insulin signalling.

Author: Lorena López Padilla

Experimental director: Dr. Stefania Carobbio

External cotutor: María del Carmen Navarro González

Academic tutor: Eduardo Bueso Ródenas

Valencia, July 2023

RESUMEN

La obesidad es una enfermedad multifactorial cuyo origen es la combinación de factores genéticos y ambientales. Se asocia con una mayor susceptibilidad a padecer otras patologías como diabetes, enfermedades cardiovasculares o el desarrollo de otros tipos diferentes de cáncer. La obesidad se produce por un desequilibrio entre la ingesta de energía y el gasto de esta. El exceso de energía se almacena en forma de grasa en los adipocitos, que son las principales células constituyentes del tejido adiposo. Los adipocitos proceden de un subconjunto multipotente de células madre mesenquimales que experimentan un proceso denominado adipogénesis por el que se convierten en células grasas maduras.

El sustrato 2 del receptor de insulina (IRS2) participa en la adipogénesis, formando parte de la ruta de señalización de la insulina. Se ha demostrado que los precursores de adipocitos en ratones knockout (KO) para IRS2 presentan una deficiencia en la diferenciación hacia adipocitos maduros.

Estudios previos han descrito el factor de transcripción zinc finger protein 423 (ZNF423) como un factor clave en el compromiso y la diferenciación de los adipocitos blancos y marrones. Datos preliminares sugieren que ZNF423 podría tener un papel aguas abajo de IRS2 en la vía de señalización de la insulina.

El objetivo de este trabajo fue estudiar si ZNF423 pudiera formar parte del proceso de diferenciación de adipocitos IRS2 KO, lo que podría llevar a identificar una posible diana para rescatar sus capacidades de diferenciación. Para ello, se llevaron a cabo diferentes experimentos.

En primer lugar, se midieron los niveles de ZNF423 mediante RT-qPCR en ratones IRS2 KO y ratones control en estado de alimentación y ayuno. Además, para comprender el comportamiento de IRS2 y ZNF423 durante la diferenciación de los adipocitos se infectaron preadipocitos de ratón 3T3-L1 con lentivirus portadores de constructos para la sobreexpresión o el silenciamiento de IRS2. Los niveles de ARNm y proteína de ZNF423 y otros genes de interés se midieron mediante RT-qPCR y Western Blot, respectivamente. Además, se realizó un análisis morfológico de los adipocitos mediante inmunofluorescencia.

El análisis morfológico mostró que los adipocitos experimentaron los cambios morfológicos típicos esperados durante la diferenciación adipocitaria. Los resultados de los experimentos con ratones muestran que los niveles de expresión de ARNm de IRS2 y ZNF423 parecen seguir el mismo patrón. Además, lo mismo pudo observarse en el experimento de silenciamiento en células 3T3-L1. Esto podría indicar que ZNF423 se encuentra aguas abajo de IRS2 en la cascada de señalización de la insulina.

PALABRAS CLAVE: IRS2, ZNF423, diferenciación adipocitaria, tejido adiposo, obesidad, lípidos, señalización de la insulina.

Autor: Lorena López Padilla

Director experimental: Dr. Stefania Carobbio

Cotutor externo: María del Carmen Navarro González

Tutor académico: Eduardo Bueso Ródenas

Valencia, julio 2023

ACKNOWLEDGMENTS

En primer lugar, me gustaría agredecer a Stefania la oportunidad de haber podido desarrollar este proyecto con el grupo I-76 y de haber podido emprender mi carrera científica. Por otro lado, muchísimas gracias a Carmen por haberme guiado en este trabajo, por toda la ayuda y por todo lo que me has enseñado. También gracias a Jaime, por haber amenizado mis días en el laboratorio y por todos los consejos que me has dado.

Gracias a mis padres, por toda la paciencia que han tenido y que tienen conmigo, porque han sido meses difíciles y gracias a ellos han podido ser un poco más fáciles. Gracias por apoyarme siempre en todo, os quiero.

Cómo no, a Mari, Fani y Jose, mi familia y mejores amigos, con los que siempre puedo contar. Gracias simplemente por ser uno de mis pilares fundamentales. Por aconsejarme, tranquilizarme y confiar en mí.

A mis biotekes, que sin vosotros llegar hasta aquí no hubiera sido posible. Todas las tardes y los findes de estudio, las videollamadas, los apuntes prestados… Pero sobre todo gracias por los momentos buenos que me habéis dado. Y pase el tiempo que pase, y aunque cada uno siga su camino, siempre vais a ser familia.

Y, lógicamente, a las personas que más me han aguantado todos estos meses, mis compañeros del Mc. Juanjo, gracias por ser un segundo padre, por los ánimos y por meterme caña. Andrea, gracias por estar ahí siempre y por ayudarme a despejarme cuando me ha hecho falta. Adri, gracias también por escucharme siempre que lo he necesitado. Y, cómo no, Paula, mil gracias por todas las quejas que has tenido que escuchar, por aguantarme tanto tanto y por ser mi compi de biblio.

Y Javi, gracias. No puedo estar más agradecida. Por haber estado cuando no he podido más, porque me has escuchado, porque has aguantado mis bajones y me has dicho que podía con todo. Y costó, pero así fue.

INDEX

FIGURE INDEX

TABLE INDEX

LIST OF ABBREVIATIONS

µg: microgram

µm: micrometre

ADIPOQ: Adiponectin

AP2: Adipocyte fatty acid-binding Protein 2

BAT: Brown Adipose Tissue

BMP4: Bone Morphogenetic Protein 4

BSA: Bovine Serum Albumin

C/EBP: CCAT/Enhancer-Binding Protein

cDNA: Complementary deoxyribonucleic acid

CT: Cycle Threshold

ctrl: control

CV: Coverslip

DEPC: Diethylpyrocarbonate

DIO: Diet-Induced Obesity

DKK1: Dickkopf WNT signalling pathway inhibitor 1

DMEM: Dulbecco's Modified Eagle Medium

EBF2: Early B-Cell Factor 2

EDTA: Ethylenediamine tetraacetic acid

FBS: Fetale Bovine Serum

FFA: Free Fatty Acid

GLUT4: Glucose Transporter type 4

HRP: Horse-Radish Peroxidase

IBMX: 3-isobutyl-1-methylxanthine

IDDM: Insulin-Dependent Diabetes Mellitus

IGF1R: Insulin-like Growth Factor 1 Receptor

IR: Insulin Receptor

IRS: Insulin Receptor Substrate

kDa: kilodalton

KO: Knockout

M: Molar

MetS: Metabolic Syndrome

mL: millilitre

mm: millimetre

mM: millimolar

MOPS: 3-(N-morpholino) propanesulfonic acid

mRNA: messenger RNA

MSC: Mesenchymal Stem Cell

Myf5: Myogenic factor 5

NIDDM: Non Insulin-Dependent Diabetes Mellitus

nm: nanometre

ov: overexpression

P/S: Penicillin/Streptomycin

PBS: Dulbecco's Phosphate-Buffered Saline

PFA: Paraformaldehyde

PI3K: Phosphatidylinositol 3-kinases

PPARγ: Peroxisome Proliferator-Activated Receptor γ

qPCR: quantitative Polymerase Chain Reaction

RIPA: Radioimmunoprecipitation

RNA: Ribonucleic acid

rpm: revolutions per minute

RT: Room Temperature

RT-qPCR: Real-Time qPCR

SD: Standard Deviation

shRNA: short-hairpin RNA

si: silencing

siRNA: small interfering RNA

UCP1: Uncoupling Protein 1

V: Volt

vs: versus

WAT: White adipose Tissue

WB: Western Blot

WISP2: WNT-1-Inducible-Signalling pathway Protein 2

WNT: *Wingless e Int*

WT: Wild Type

1. INTRODUCTION

1.1. Obesity

Obesity and overweight are an abnormal or excessive accumulation of fat that can be harmful to health. Since 1975, obesity has tripled worldwide. In 2016, more than 1.9 billion adults aged 18 and over were overweight, of which more than 650 million were obese (World Health Organization, 2021).

Obesity poses a serious danger to public health since it negatively affects almost all physiological systems of the body. It raises the chance of having a number of complications that have an adverse impact on quality of life, productivity at work, and healthcare expenditures, including diabetes mellitus, cardiovascular disease, various malignancies, a variety of musculoskeletal problems, and poor mental health (Chooi et al., 2019).

Furthermore, obesity appears very frequently with other three pathogenic states, more than it appears for itself. These are insulin resistance, dyslipidaemia, and hypertension. All together with obesity they are known as the Metabolic Syndrome (MetS) or Syndrome X (Virtue & Vidal-Puig, 2010).

Obesity is a multifactorial disease (Chooi et al., 2019) determined by an imbalance between energy intake and energy expenditure. Adipocytes are a component of the biggest endocrine unit in the body, the adipose tissue. They must store this extra excess as fat. Adipocytes' fat is oxidized to liberate free fatty acids (FFAs) for gluconeogenesis and energy consumption when the body needs to expend energy (Schelbert, 2009).

There are two principal forms in which adipose tissue can grow. It is called hypertrophy when existing adipocytes increase size and hyperplasia when new adipocytes are created from the differentiation of resident precursors (preadipocytes). Early in life is when most adipocytes are determined, and this number remains largely steady throughout adulthood (Spalding et al., 2008). Nevertheless, new adipocytes can develop from the differentiation of preadipocytes over a sustained caloric excess and can support the growth of adipose tissue. The equilibrium of these expansion ways has a significant effect on metabolic health. Unbalance can increase systemic insulin resistance, hypoxia and adipose tissue inflammation (Halberg et al., 2009). However, small adipocytes are crucial for reversing the metabolic decrease brought on by obesity and they are associated with a lower risk of acquiring diabetes (Ghaben & Scherer, 2019).

Finding new, effective, and secure anti-obesity drugs is always needed due to the present anti-obesity treatments' limited efficacy, potential side effects, and medication interactions. Some potential anti-obesity actions of natural products are the induction of apoptosis, cell-cycle halt or delayed advancement, and interference with transcription factor cascade or intracellular signalling pathways at the early stage of adipogenesis (Jakab et al., 2021).

1.2. Adipose tissue

There are two different types of adipose tissue, brown (BAT) and white (WAT). BAT is mainly responsible for non-shivering thermogenesis in response to cold stress or β-adrenergic stimulus, while WAT plays a crucial role in lipid homeostasis and maintaining energy balance (Jakab et al., 2021). Along the body axis, WAT is distributed in many depots, including visceral, subcutaneous, and perigonadal. Brown adipocytes can also be seen as intermittent foci in skeletal muscle and inside the white adipose tissue depots, such as subcutaneous and peritoneal. BAT preferentially forms distinct depots in the interscapular area and surrounding the aorta in mice. Adult humans can identify distinct BAT depots in the cervical-supraclavicular region that resemble mouse depots and are known as canonical BAT. The brown in white ('brite') or 'beige' adipocyte is a third kind of adipocyte that has been discovered (Carobbio et al., 2013). While BAT originates embryonically, postnatal life is when browning of WAT begins. BAT is abundant throughout childhood but comes back in maturity. However, adult humans have been shown to have brown and beige adipocytes, which grow following exposure to cold (Kajimura et al., 2008). Despite coming from different developmental sources and being situated in different parts of the body, they share a lot of aspects (Rui, 2017).

WAT is a dynamic organ that accomplishes several important physiological processes (Sarjeant & Stephens, 2012). WAT main function is to store excess nutrients and mobilise them to other organs when needed. It also act as mechanical cushion to protect internal organs like heart, adrenal glands, kidneys, and ovaries as well as anatomical areas like the palms, buttocks, and heels (Hafidi et al., 2019).

Until recently, white adipose tissue was viewed as a simple lipid depot but now it is considered as an important endocrine organ that regulates metabolic balance through the secretion of a variety of hormones (Clavijo et al., 2007). To avoid lipotoxicity caused by accumulation of ectopic lipids in other tissues including the liver, heart, and muscle, adipose tissue's main job is to sequester them. Insulin resistance, inflammation, and cell death are all caused by lipotoxicity, which disrupts membrane fluidity, membrane transport, receptor signalling, and the release of lipidic mediators and oxygen metabolites (Hafidi et al., 2019). In fact, adipose tissue is crucial for whole-body insulin sensitivity and energy homeostasis (Lefterova & Lazar, 2009).

Although adipose tissue hosts different cell types such as endothelial cells, blood cells, fibroblasts, pericytes, preadipocytes, macrophages, and other immune cells, mature adipocytes are the main constituent cells (Sarjeant & Stephens, 2012).

1.2.1. White adipose tissue (WAT) and brown adipose tissue (BAT)

Adipocytes can be derived from different mesenchymal precursors. Brown adipocytes are derived from mesenchymal precursors which express Myogenic factor 5 (Myf5), while white adipocytes are derived from those which not express Myf5 (Figure 1) (Sarjeant & Stephens, 2012).

Adipocytes that mainly form WAT are large and spherical adipocytes that are closely packed, also known as unilocular fat cells because when they are mature, almost all the cell is filled by a big lipid droplet that contains triglycerides. A loose connective tissue

that is highly vascularized supports these cells which have a size range from 30-130 µm in diameter. There is a relation between the volume of the adipocytes and their functionality. The larger they are, the higher metabolic activity and more chemoattractants secretion for immune cells they have (Wronska & Kmiec, 2012)

On the other hand, multilocular adipocytes or cells with various lipid droplets can be found in BAT. The sympathetic nervous system innervates and well-vascularizes brown adipose tissue. Brown adipocytes often have an ellipsoid form, measure 15 to 50 mm in size (Sarjeant & Stephens, 2012). It is highly mitochondrial and specialized in heat production, which results in energy expenditure while WAT is the primary site of energy storage (Vázquez-Vela et al., 2008).

The inner mitochondrial membrane of BAT is characterised by the presence of uncoupling protein 1 (UCP1), which is regulating BAT thermogenic activity. Leptin, the nuclear corepressor RIP140, and matrix protein fibrillin-1 are more highly expressed in WAT than in BAT (Saely et al., 2011). Leptin is a hormone mostly expressed by adipose tissue which has anti-obesity properties. By acting on the brain, its main function is to reduce appetite and promote energy expenditure. Although it is regulated by different factors, leptin's nutritional control is partially regulated by insulin, since leptin rises in response to insulin stimulation and falls in reaction to low insulin levels (Ahima & Flier, 2000). Fibrilin-1 is a glycoprotein which regulates adipocyte metabolism more than proliferation, via giving adipocytes mechanical support or by activating signalling pathways as a result of interactions between adipocytes and fibrillin-1 (Muthu & Reinhardt, 2020).

Other differences are that while large amounts of WAT are related with an increased risk of suffering obesity-associated disorders, large amounts of BAT are associated with a decrease of the risk of suffering obesity-related disorders. Also, WAT increases with age relative to total body weight whereas BAT decreases (Saely et al., 2011).

1.2.2. Beige adipocytes

Beige adipocytes are sporadic thermogenic adipocytes inducible forms found in WAT depots. These and brown adipocytes have in common the characteristics of having many cristae-dense mitochondria that express UCP1 and multilocular lipid droplets (Figure 1). Therefore, their function is thermogenesis to conserve body temperature and, also, they have a beneficial impact on the body's overall glucose control by acting as a sink sequestering glucose from the blood stream and using it as fuel, what could be useful in the management of type 2 diabetes (Ambele et al., 2020). The 'browning' or 'beigeing' of WAT is how it is called the event that consists in the biogenesis of beige adipocytes in WAT which occurs as a result of the response of these cells to environmental factors and outside influences, including as exercise, persistent cold acclimation, peroxisome proliferator-activated receptor γ (PPARγ) or β3-adrenergic receptor agonist therapy, cancer cachexia, and tissue damage (Ikeda et al., 2018).

Because of their capacity for releasing energy and a potential ability to distinguish themselves from white adipocytes, beige adipocytes have recently received particular attention. Knowing the factors that influence beige adipocyte cell development may be

crucial for the development of new paths for the treatment of metabolic illnesses (F. Lizcano, 2019).

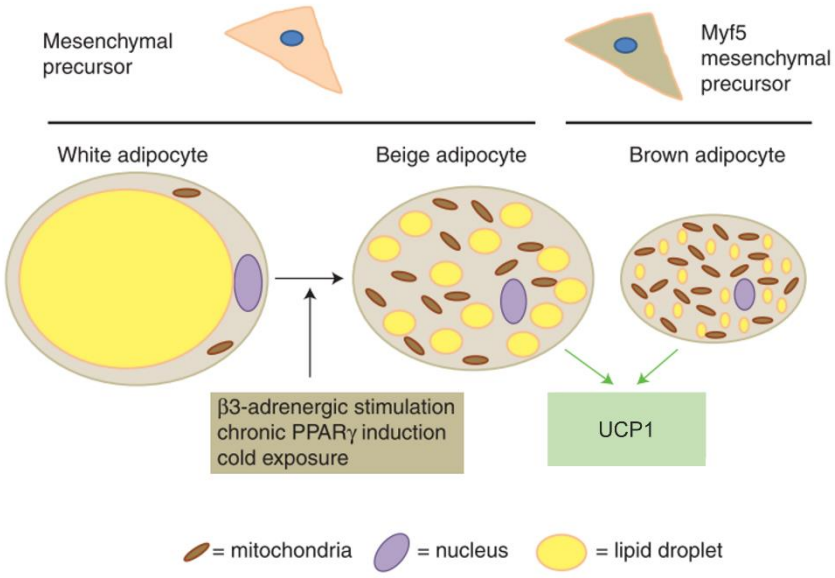

Figure 1. The different types of adipocytes. *Brown and white adipocytes have different origins. Different conditions stimulate the browning of WAT. Beige and brown adipocytes have many cristae-dense mitochondria that express UCP1 and multilocular lipid droplets, while white adipocytes contain a large lipid droplet. Adapted from Sarjeant & Stephens, 2012.*

1.2.3. Adipocyte differentiation and adipogenesis

Preadipocytes undergo a process called adipogenesis in order to develop into adult fat cells, which play an important metabolic and endocrine role (Clavijo et al., 2007). There is a steep increase in the number of adipocytes and during infancy (from birth to 6 months) and its growth stabilise determining the amount and ability of adipose tissue to store lipids in adults (Jakab et al., 2021).

Adipocytes develop from many, dynamic, and widely dispersed lineages. Commitment and terminal differentiation are the two distinct stages of differentiation. During commitment, mesenchymal stem cells (MSCs) commit to become preadipocytes, after which they proceed through terminal differentiation to become mature adipocytes through a process called adipogenesis. When MSCs commit to the adipocyte lineage and lose the ability to develop into other cell types (osteocytes, chondrocytes, myocytes, etc.), they go through morphological and functional changes. These processes are the result of the action of a wide variety of transcription factors and genes, as well as various signalling pathways (Ambele et al., 2020).

In preadipocytes commitment, the wingless-type mammary tumour virus integration site family (WNT) signalling pathways crucial. The maintenance of uncommitted and undifferentiated progenitor cells highly depends on this signalling pathway. Hence, it is necessary that it ends in order for the adipogenic differentiation begins. Dickkopf family proteins like inhibit the WNT signalling pathway to induce preadipocytes commitment

and differentiation. One example is the Dickkopf WNT-signalling pathway inhibitor 1 (DKK1). However, it needs the action of other factors. For example, it has been demonstrated that bone morphogenetic protein 4 (BMP4) is enough to induce adipocyte commitment. By activating the transcription factor SMAD4, BMP4 activates PPARγ transcriptional expression, inducing terminal differentiation (Longo et al., 2019) (Figure 2).

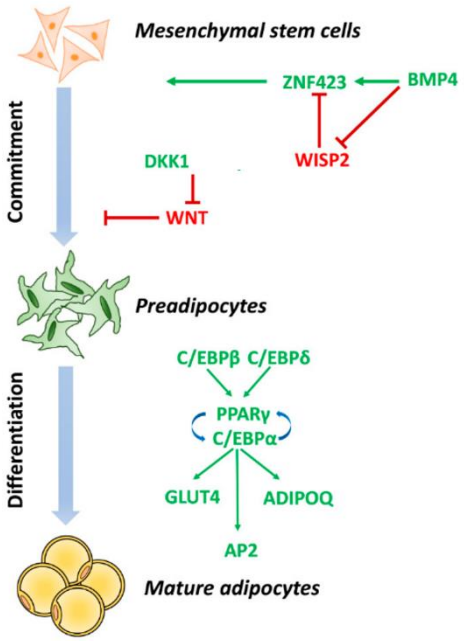

Figure 2. Molecular regulation of adipogenesis. *Different pathways, genes and transcription factors are involved in adipogenesis, by stimulating or inhibiting it. Adapted from Longo et al., 2019.*

It has been demonstrated that PPARγ and CCAAT/enhancer-binding protein (C/EBP) α are crucial in the process of adipogenesis *in vivo* and *in vitro*. These, together with other transcription factors and epigenetic regulators activate genes for the differentiation of preadipocytes toward mature adipocytes. PPARγ and C/ EBPα acts together to promote this differentiated state. Both are induced by C/EBPβ and C/EBPδ which act in the early phase of adipogenesis (Lee et al., 2019). Different key genes are expressed once PPARγ and C/EBPα are activated. This includes glucose transporter type 4 (GLUT4), adipocyte fatty acid-binding protein 2 (AP2), and adiponectin (ADIPOQ). All of them are crucial for regular adipocyte function which includes insulin sensitivity (Longo et al., 2019) (Figure 2).

1.3. *In vivo* models of obesity

Prevalence of obesity makes necessary its prevention and treatment. For that reason, animal models sharing human characteristics of obesity and its comorbidities have been developed (Lutz & Woods, 2012).

Different types of animals can be used in obesity research such as non-mammalian, large animals, or rodent models. However, there are several disadvantages and advantages for each one what make rodent animals the most used models. Their usefulness is explained by the fact that their physiology is more similar to humans than the one of non-mammalian models, as well as by their tiny size, high breeding capacity, and brief life cycle (Kleinert et al., 2018).

Animal models may be categorized into several distinct groups, the two main ones being those based on wild type animals exposed to obesogenic conditions against those based on mutations or gene-specific alterations. Rather than the action of a single gene, the development of obesity depends on the coordinated activity of several genes (Lutz & Woods, 2012).

The creation of polygenic diet-induced obesity (DIO) models, which are frequently employed to research the polygenic origins of obesity, has made significant progresses (Barrett et al., 2016).

The more appropriate animal model selection depends on the study and its objective. For example, DIO models are useful for therapeutic studies. To determine if a potential therapy targets a particular gene or pathway in vivo, it may be preferable to use genetically modified animals. They may also be utilized to investigate the possible roles of specific molecular targets and pathways in the physiology of food intake and obesity (Lutz & Woods, 2012).

1.4. *In vitro* models of adipocytes

Cellular models have allowed the understanding of a lot of molecular pathways regulating adipocyte development. There are several cellular models, and they can be classified depending on the lineage commitment they can undergo, their proliferative ratio or the tissue of origin from which they have been isolated. One type is the mesenchymal stem cells which, thanks to its multipotency can differentiate into variety of lineages not only adipocytes i.e neurocytes, chondrocytes or osteoblasts (Thomson et al., 1998). Another cellular model with more restricted capability to commit are the preadipocytes. 3T3-L1 and 3T3-F442A are the most used preadipocyte cell lines, which are isolated from the Swiss 3T3 mouse embryos (Armani et al., 2010) (Zhang et al., 2020).

3T3-L1 cell line can undergo a fairly high number of passages and is homogenous in terms of cell population, providing a homogenous response following treatments and changes in experimental conditions (Poulos et al., 2010). The function of various genes related to adipogenesis, adipokine production or adipokines secretion have been studied through gene silencing methods in 3T3-L1 cells. This include siRNA and shRNA transfected into the cells using different techniques (lentivirus, adenovirus and plasmid electroporation) (Ruiz-Ojeda et al., 2016).

Another murine model is the C3H10T1/2 stem cell line. It comes from 14-to 17-day C3H mouse embryos (Reznikoff et al., 1973). Like all other cell lines, they do not differentiate into adipocytes if they are not in an environment with specific differentiation-promoting components. However, in the presence of BMP4, their commitment to adipocyte differentiation is induced (Tang et al., 2004).

Preadipocyte cells from humans with Simpson-Golabi-Behmel syndrome (SGBS) are one of the few human cell lines accessible. The function of human adipocytes has so far been studied using these cells among other models such as primary adipocytes and adipose tissue stem cells. In contrast to primary human preadipocytes, which rapidly lose their capability for differentiation when replicated in vitro, the SGBS maintain their capacity to differentiate even after proliferation for up to 50 generations (Fischer-posovszky, 2008).

1.5. Insulin and diabetes

Insulin is an important molecule in metabolic physiology. It is released by β-cells present in the islets of Langerhans of the pancreas when there is an increase of blood glucose concentration. Insulin released into the blood is directed to its principal target tissues which are fat, liver and muscle (Myers & White, 1996) where it binds to its receptor. This results in the activation of a signalling pathway, which has two functions: first, to stimulate the flow of nutrients from the bloodstream to these tissues, including glucose, amino acids, and fatty acids; and second, to promote the conversion of these nutrients into storage molecules, including glycogen, protein, and lipids (Lizcano & Alessi, 2002). Also, the secretion of insulin inhibits hepatic glucose production (Withers et al., 1998).

Insulin and insulin-like growth factor 1 receptors (IR/IGF1R) are some of the receptors involved in the insulin-signalling pathway (Taniguchi et al., 2006). They regulate growth, differentiation, and metabolism. These receptors are activated when the ligand binds to them at the cell surface. Then, they undergo a conformational change and tyrosine residues on their cytoplasmic subunits are auto phosphorylated. This activates the recruitment and phosphorylation of insulin receptor substrate (IRS) proteins and other substrates, which promote the downstream signalling. The PI3K-AKT and Ras-Raf-MAPK pathways, which regulate metabolic balance and growth among others, are two important pathways that this cascade stimulates (Manohar et al., 2020).

Insulin is related with diabetes mellitus, one of the most common metabolic disorders. There are two types of diabetes. Type I diabetes or insulin-dependent diabetes mellitus (IDDM) and type II diabetes or non-insulin-dependent diabetes mellitus (NIDDM). High amounts of blood glucose are a hallmark of both types. However, IDDM is due to a failure in the synthesis of insulin whereas, in NIDDM, target tissues become resistant to the effects of insulin (Myers & White, 1996).

Risk factors such as hyperglycaemia, dyslipidaemia, and hypertension are caused by insulin resistance, which also causes compensatory hyperinsulinemia. Furthermore, it promotes the development of type 2 diabetes along with cardiovascular diseases, non-alcoholic fatty liver disease, and other illnesses (MetS) (Copps & White, 2012).

1.5.1. Insulin receptor substrate 2 (IRS2)

IRS are intracellular substrates of IR/IGF1R. There are six different IRS named as IRS 1-6. IRS1 and IRS2 are both ubiquitously expressed. IRS3 is mostly restricted to adipocytes and the brain, while IRS4 is predominantly expressed in embryonic tissues or cell lines (Taniguchi et al., 2006).

Each IRS-protein consists of a phosphotyrosine-binding domain followed by a highly conserved NH_2-terminal pleckstrin homology domain, which together, tie IRS proteins to the active insulin or IGF-1 receptors. The regulatory subunit of the lipid kinase phosphatidylinositol 3-kinase (PI3K), Grb2, nck, and SHP2 are among the effector proteins that bind to the SH2 domains of IRS-proteins, which include 8–18 possible tyrosine phosphorylation sites in a variety of amino acid sequence motifs. The impact of insulin on glucose transport, glycogen synthesis, protein synthesis, lipolysis, and the regulation of hepatic gluconeogenesis is mediated by a network of serine-threonine kinases, which are activated by PI3K (Burks & White, 2001).

IRS proteins has a significant role in the interaction between insulin resistance and cell dysfunction in type 2 diabetes. Most of obese people don't develop diabetes because hyperinsulinemia makes up for decreased insulin action in peripheral tissues. However, it has been demonstrated that deletion of IRS2 in mice leads to insulin resistance and causes impairment of cell development and function (Burks & White, 2001).

On another hand, it has been demonstrated that IRS2 plays a crucial role in adipogenesis. A study revealed that lack of IRS2 along with IRS1 significantly reduces the expression of PPARγ and C/EBPα during adipogenesis at both the mRNA and protein levels. As a result, IRS2 has a critical function in the expression of adipose-specific transcriptional factors (Miki et al., 2001).

1.6. Zinc finger protein 423 (ZNF423)

Zinc finger protein 423 (ZNF423) is a nuclear protein. It is a member of the Kruppel-like C2H2 zinc finger proteins family. ZNF423 is a transcription factor which binds to DNA by making use of different zinc fingers domains in various signalling pathways (NIH, 2023). A zinc finger is a folded structure consisting of approximately 30 amino acids. These zinc fingers are stabilised by the coordination of zinc ions at their centre. Each zinc finger contains a specific combination of amino acids that determines its three-dimensional structure and its ability to recognise and bind to specific DNA sequences (Chaible et al., 2017).

ZNF423 acts in adipogenesis as a transcriptional coregulator of PPARγ (Dang et al., 2022). ZNF423 is essential for the early development of white and brown adipose tissue *in vivo* and is necessary for adipocyte differentiation *in vitro* (Gupta et al., 2012).

Moreover, it has been demonstrated that ZNF423 has a crucial role for suppression of the thermogenic gene program ('beigeing') in white adipocytes (Shao et al., 2021) maintaining their identity by antagonizing the transcription factor early B-cell factor 2 (EBF2) (Lee et al., 2019).

As shown in figure 2, BMP4 induces nuclear entry of ZNF423. ZNF423 is in an intracellular complex with wnt-1inducible-signalling pathway protein 2 (WISP2), which retains it in the cytosol. BMP4 dissociates this complex, permitting to ZNF423 to enter the nucleus. As a result, PPARγ transcription is activated, and precursor cells are committed to the adipocyte lineage. The development of hypertrophic obesity and its related metabolic effects, including insulin resistance and type 2 diabetes, are favoured by the inability to separate the WISP2/ZNF423 complex (Longo et al., 2019).

However, the role of ZNF423 in adipocyte differentiation needs to be further investigated.

2. HYPOTHESIS AND OBJECTIVES

Previous studies were carried out in white adipose tissue from IRS2 knockout (KO) mice. They have demonstrated that adipocyte precursors from these mice show an impairment in the differentiation into mature adipocytes. There is an accumulation of progenitors, but they do not differentiate.

ZNF423 is a transcription factor that has been described in the literature as playing a key role in white and brown adipocytes commitment and differentiation. Preliminary data suggest that ZNF423 could have a role downstream IRS2 in the insulin signalling pathway.

Given these preliminary data, the hypothesis is that ZNF423 could rescue the impairment of IRS2 KO adipocytes differentiation process.

To study this, the objectives are as follows:

1. Profiling ZNF423 by RT-qPCR in IRS2 KO and control mice in fed and fasted states.
2. Investigate the consequences of IRS2 overexpression or silencing in the adipocyte differentiation process and studying the ZNF423 response at mRNA level by RT-qPCR.
3. Study the consequences of IRS2 overexpression or silencing in the adipocyte differentiation process and studying the ZNF423 response at protein level by Western Blot analysis.
4. Visualizing the effects of IRS2 overexpression or silencing on adipocyte morphology by immunofluorescence.

3. MATERIALS AND METHODS

3.1. IRS2 (KO) mice

Samples of adipose tissue from $IRS2^{-/-}$ mice were provided by collaborators in order to study the ZNF423 profile under different nutritional conditions. These were fed and fasting male and female IRS2 KO mice.

ZNF423 mRNA levels were measured by Real Time qPCR (RT-qPCR)18S, 36B4, PPIA, RPL19 (supplementary table S1) were the genes chosen as housekeeping and used to normalise ZNF423.

3.2. Cell lines

For this project, 3T3-L1 preadipocytes (CL-173™) (ATCC) were chosen. They are a fibroblast cell line isolated from a mouse embryo.

Different cells lines were generated in the laboratory in order to study ZNF423 behaviour during adipocyte differentiation.

First, 3T3-L1 stable cell line overexpressing IRS2 was generated by lentivirus infection. The lentivirus was the Rlv-EF1-tag-Mirs2, which overexpress the human IRS2 protein. The Rlv-EF1-GFP lentivirus, which express GFP protein, was used as a control of the infection. Both lentiviruses are from Vectalys, and they were generated from lentiviral based vectors expressing a type A transgene.

On another hand, a stable cell line silencing IRS2 was generated by lentivirus infection. The lentivirus for silencing IRS2 is called GFP-sh2-Mirs2 (sh135). As control for the infection, we used a lentivirus called, GFP-ctrl (sh726). Both lentiviruses express GFP. In order to have a uniform population of cells in which all the cells had integrated the lentivirus, they were selected by cell sorting (using GFP expression). In this way, we obtained 3 different cell populations. One of them was the control cells that were not silenced for IRS2 but underwent lentivirus infection (GFP positive cells). The other two populations did silence for IRS2 and, consequently expressed GFP, but one of them expressed low amounts of GFP protein. However, we only performed expression analysis on control cells and IRS2 silenced cells expressing the highest amount of GFP. Those that did not express any GFP were discarded.

3.3. Cell culture

3.3.1. Culture media

Table 1. 3T3-L1 growth and differentiating media.

Dulbecco's Modified Eagle's Medium (DMEM)– high glucose (25 Mm) (Sigma-Aldrich, D5796)
10% Fetal Bovine Serum (FBS) (Labclinics, FBS-11A) 1% Penicillin/Streptomycin 10000 U/mL (P/S) (Sigma-Aldrich, P0781) 1% L-Glutamine 200 Mm (Sigma-Aldrich, G7513)

Table 2. 3T3-L1 induction cocktail.

Suppliment	[final]
3-isobutyl-1-methylxanthine (IBMX) (Sigma-Aldrich, I-7018)	0,5 Mm
Dexamethasone (Sigma-Aldrich, D-1881)	1 µM
Insulin (Sigma-Aldrich, I-5500)	5 µg/mL

3.3.2. Growth and differentiation protocol

Cells were stored in vials in liquid nitrogen. To defrost cells, they were incubated at 37ºC. Once they were defrosted, it was necessary to work under aseptic conditions (laminar flux hood type 2A). They were transferred to a falcon tube containing 10 mL of culture media (table 1) that had been previously attempered at 37ºC in a water bath. The cells were centrifuged using the Centrifuge 5415 R (Eppendorf), at 1200 rpm for 5 minutes. Then, the medium was removed, and cells were resuspended in 1 mL of medium (table 1) and placed in a T-75 flask (CORNING, 00430641U).

Medium was replaced with fresh medium every 3 days. In addition, the cells were sub-cultured before they became confluent, as this would lead to a loss of cell differentiation

capacity. To pass the cells the medium was removed, and they were washed with 5 mL of Dulbecco's Phosphate-Buffered Saline 1x (PBS) (Labclinics, L0615-500). The PBS was immediately removed, and the cells were detached with 2 mL of trypsin 0'05% ethylenediamine tetraacetic acid (EDTA) (Sigma, 25300054) for three minutes. Then, 2 mL of medium was added. These 4 mL containing medium, trypsin and cells were transferred to a 15 mL falcon tube and centrifuged at 1200 rpm for 2 minutes. Then, the supernatant was removed, and the pellet was resuspended in approximately 8 mL of medium. Then, culture medium was added to a new T-75 flask and 75 000 cells/flask were seeded.

To start the preadipocyte differentiation, 55 000 cells/well were seeded in growth medium (table 1) in a 12 well plate. When the cells were confluent, which took around 48 hours, the medium was changed.

After 48 hours, the differentiation process was started. The cells were incubated in the differentiation medium (table 1) containing the induction cocktail (table 2). This was the day 0 of the differentiation.

On day 3 and day 6 the medium was changed. This medium contained the differentiating medium and 5 µg/mL of insulin (Sigma-Aldrich, I-5500).

3.3.2.1. RNA and protein collection

Cells were collected at different days during the differentiation process (D0, D1, D3, D5, D7 and D9) to extract RNA and proteins. For that, the medium was removed. Then, washed with 500 µL/well of PBS and later 250 µL/well of trypsin 0'05% EDTA was added and incubated at room temperature for three minutes. After, the same amount of medium was added, and the cells were collected in Eppendorf tubes by resuspending them. They were centrifuged for 2 minutes at 1200 rpm. Once finished, the medium was removed, and the cells were kept at -80ºC.

3.3.2.2. Cells fixation for immunofluorescence

Moreover, during this process, the cells were fixed in different days (D1, D3, D5, D7, D9). The cells were grown on coverslips in a 12 well plate. In order to fix them, the culture medium was removed. Then, the coverslips were transferred to another 12 well plate with 1 mL of PBS. Then, the PBS was immediately removed, and the cells were fixed by adding 500 µL of paraformaldehyde (PFA) 4% in PBS (Fisher Scientific, J61899.AP). After 15 minutes, the PFA was removed, and each coverslip was washed three times with 1 mL of PBS. Finally, the coverslips were maintained with 2 mL/well of PBS at 4ºC until the immunostaining was performed.

3.4. Analysis of mRNA expression

3.4.1. RNA extraction and quantification

The cells were homogenised in 1 mL of TRItidy G™ (PanReac AppliChem, A4051,0200) by pipetting the suspension up and down several times. Then, they were incubated for 5 minutes at room temperature (RT) and 200 µl of Chloroform (PanReac AppliChem, 141252.1611) were added to the lysate and mixed by vortexing with the Fisherbrand™ZX4 vortex (Thermo Fisher Scientific, 13284769). At this moment, the

samples were incubated for 10 minutes at RT to improve the purity of the RNA. After a centrifugation at 12 000 g for 15 minutes at +4ºC, the upper aqueous phase was transferred to a new microtube, and the same volume of Isopropanol (Thermo Fisher Scientific, 10477070) was added to precipitate the RNA. These tubes were incubated in the freezer at -20ºC overnight. The next day, the samples were centrifuged at 12 000 g for 15 minutes at +4ºC. The pellet was kept and washed with 1 mL of ethanol 70%, made from absolute Ethanol (PanReac Applichem, A8075.1000PE), by vortexing and centrifuge at 7500 g for 5 minutes at 4ºC. The RNA was washed with 1 mL of ethanol 70% by pipetting the suspension up and down and centrifuged at 7 500 g for 5 minutes at +4ºC. The supernatant was removed, and the RNA was air-dried. Once dried the RNA was resuspended in 30 µl DEPC-treated water (Thermo Fisher Scientific, 11528616).

The RNA obtained was quantified in the NanoDrop™ ND-1000 spectrophotometer (Thermo Fisher Scientific). The RNA concentration of each sample was measured using absorbances values at 260nm (A260). Purity was determined with the 260/280 and 260/230 ratios.

3.4.2. RT-qPCR

The expression of the genes of interest was measured through RT-qPCR. This method allows to quantify the amount of mRNA by amplifying the specific mRNA of the gene of interest using specific primers (supplementary table S1).

For each sample, the cDNA was synthetised from 0.5 µg of RNA in 10 µL of DEPC-treated water. Also, 4 µL of 5X PrimeScript™ RT Master Mix (Takara, RR036B) with 6 µL of RNAse-Free Water (Takara, 9012) were added.

Then, the reverse-transcription reaction was performed in the Mastercycler Pro Thermal Cyclers (Eppendorf, EP631100010-1EA). This procedure consists of a 15-minute reverse transcription phase at 37°C, followed by a 5-second inactivation stage at 85°C. The cDNA was then kept at -20ºC until use.

The cDNA obtained was diluted (1:100). The amplification was performed in the 384 well PCR Microplate (Axygen, G0PCR-384-LC480-W). In each well 5 µL of diluted cDNA were added. Also, 4.92 µL of TB Green *Premix Ex Taq* II (2x) (Takara, RR420W) and 0.04 µL of each forward and reverse primers (50 µM) were added. The qPCR was performed in the LightCycler® 480 II (Roche) and three replicates for sample were used. This amplification protocol was as follows: first, a pre-incubation of 2 minutes at 95ºC. Then, 45 amplification steps. Each one of them consisted in 30s at 95ºC to denaturalise the RNA, 30 seconds at 60ºC to hybridise the primers and 30 seconds at 72ºC to amplify the RNA. Finally, a melting curve was generated. First, 15 seconds at 95ºC. The temperature then dropped to 60°C and rose again to 97°C progressively for 40 seconds.

The LightCycler program gave a cycle threshold (CT) value for each triplicate. CT value represents the PCR cycle where the cDNA is detected over the background noise. The average for each sample and gene was calculated. The $2^{-\Delta\Delta CT}$ method (Livak & Schmittgen, 2001) was used to calculate the relative expression.

3.5. Analysis of protein expression

3.5.1. Protein extraction and quantification

First, one pill of Protease Inhibitor Mini Tablets (Thermo Scientific, A32955) was added to 1 mL of RIPA (radioimmunoprecipitation) lysis buffer 10x. This buffer was made of Sodium chloride (NaCl) 1.5 M (Merck, 1.06404.1000), Nonidet 10%, Tris 500 mM (Thermo Fisher Scientific, 10376743), Deoxycholate-Na 5% (Sigma-Aldrich, 30970) and Sodium Dodecyl Sulphate (SDS) 1% (Thermo Fisher Scientific, 28312). After that, the pellet was resuspended in 100 µl of RIPA 1x and left on ice for 30 minutes, vortexing every 5 minutes to promote the lysis of the sample.

The next step consisted in spinning the samples 15-20 minutes at maximum speed at 4ºC and collecting the supernatant into fresh tubes.

The method used to quantify the proteins amount was the Bradford method, based on a colorimetric assay. For that, a 96-well plate was employed. First, 200 µL of Bradford reagent (Sigma-Aldrich, B6916-500ML) were added to each well. In order to do the standard curve, 5 µL of bovine serum albumin (BSA) (VWR®, Avantor) standards were added, each one in triplicate. Concentrations were 0, 25, 125, 250, 500, 750, 1000 µg/mL. Then, 1 µl of each diluted sample was added to each well in triplicate. This plate was incubated in the darkness for 5 minutes.

The absorbances were measured at 595 nm in the Victor2 Microplate Reader (Wallac 1420). By comparing the absorbance values obtained for each sample to the one of the standard curve, it was possible to extrapolate the protein concentrations of the samples.

3.5.2. Western Blot analysis

First, the samples were prepared as follows. 20 µg of protein were mixed with 4X LDS Sample Buffer (Thermo Fisher Scientific, NP0007) and 10% Sample Reducing Agent 10X (Thermo Fisher Scientific, NP0009) and MiliQ water to a final volume of 20 µl. Then, the samples were boiled for 5 minutes at 95ºC to denature them, left on ice for 5 minutes and centrifuged for 1 minute at maximum speed.

Proteins were separated using a gradient polyacrylamide gel (4-12% Bis-Tris Midi Gel (Thermo Fisher Scientific, 10267072)). The gel was run using the tank of electrophoresis Xcell4 Surelock™ Midi-Cell system (Thermo Fisher Scientific, WR0100) filled with 1 litre of MOPS (3-(N-morpholino) propanesulfonic acid) Running Buffer made up with MOPS SDS 20X (Thermo Fisher Scientific, NP0001). Then, the comb was removed and 435 µL of Antioxidant (Invitrogen by Thermo Fisher Scientific, NP0005) was added. The gel was run for 1 hour at 200 V in the PowerPac™ Basic Power Supply (BIO RAD).

Once the separation was finished, proteins in the gel were transferred to a nitrocellulose membrane using the iBlot™ 2 system (Thermo Fisher Scientific, IB21001) and using iBlot®2 NC Regular Stack (Thermo Fisher Scientific, IB24001) for 10 minutes. This transfer consisted in a four-step program, whose voltage and duration are shown in table 3.

Table 3.Voltage (V) and time (minutes) of the transfer program from the gel to a nitrocellulose membrane.

Step 1	Step 2	Step 3	Step 4
20 V 01:00	23 V 04:00	25 V 02:00	25 V 03:00

Once the transfer was completed the membrane was washed in MiliQ water and briefly in PBS-T. The PBS-T is composed of PBS 1X prepared from PBS 10X (Labclinics, X0515-500) and 500 µL of Tween® 20 (Sigma-Aldrich, P1379) in 1 litre. Then, the membrane was blocked for one hour at room temperature in PBS-T 5% milk on shaker for avoiding unspecific bindings. Then, it was washed in PBS-T and incubated overnight at 4ºC with the primary antibody diluted in PBS-T 3% BSA with NaAzide 0,8% on a shaker. Different primary antibodies were used to detect the proteins of interest (table 5).

After incubation, the membrane was washed three times with PBS-T on a shaker for 10 minutes each time. Then, it was incubated with the secondary antibody diluted in PBS-T 5% milk for 1-2 hours on shaker at RT. Once incubated, the membrane was washed in the same way as with the primary antibody. Two different secondary antibodies (table 4) were used for the chemiluminescent detection.

Finally, membrane was incubated for 5 minutes with the horse-radish peroxidase (HRP) substrate and developed using the chemiluminescence and spectral fluorescence system Alliance Q9 Advanced (Uvitec Cambridge).

Table 4. Primary and secondary antibodies used in the immunodetection.

	Antibody	Dilution	Species
Primary antibodies	Anti-β-actin (abcam, ab16039)	1:2000	Rabbit
	Anti-β-tubulin (Santa Cruz Biotechnology, sc-5274)	1:2000	Rabbit
	Anti-FLAG Tag (Sigma-Aldrich, borrowed)	1:1000	Mouse
	Anti-GAPDH (Sigma-Aldrich, MAB374)	1:1000	Mouse
	Anti-GFP (Rockland, 600-401-215)	1:1000	Rabbit
	Anti-IRS2 (Sigma-Aldrich, MABS15)	1:1000	Mouse
	Anti-Periplin 1 (D418) (Cell Signaling Technology, #3470)	1:1000	Rabbit
	Anti-PPARγ (Santa Cruz Biotechnology, sc-7273)	1:500	Mouse
	Anti-ZNF423 (Sigma-Aldrich, ABN410)	1:500	Rabbit
Secondary antibodies	Anti-mouse IgG, HRP-linked (Cell Signaling Technology, 7076)	1:5000	
	Anti-rabbit IgG, HRP-linked (Cell Signaling Technology, 7074)	1:5000	

3.6. Adipocyte morphological analysis

3.6.1. Staining cells and immunofluorescence

The coverslips with the fixed cells were washed with 1 mL of PBS 1X. Then, the cells were permeabilized with 500 µL of PBS 1X 0'1% Triton™ X-100 (Sigma-Aldrich, X100). After 10 minutes, they were washed 3 times with 1 mL of PBS 1X. The first time fast, the other times for 5 minutes. Then, they were blocked during 30 minutes with 500 µL of PBS 1X BSA 2%.

After that step, 100 µL of primary antibody (anti-PLIN1, 1:200 dilution) in blocking solution was added. The coverslips were incubated overnight in a wet chamber.

The following day, the antibody was removed. Then, the coverslips were washed three times with PBS 1X. The secondary antibody (Anti-Rabbit IgG (H+L), CF™ 647, Sigma-Aldrich, SAB4600184) was prepared in blocking solution at a dilution of 1:500 and HCS LipidTOX™ Red Neutral Lipid Stain (Thermo Fisher Scientific, H34476) at a dilution of

1:200. LipidTOX was added to stain the lipid droplets. 100µL of this solution were added to each coverslip. Then, the coverslips were incubated for 60 minutes in the dark.

The LipidTOX™ was removed and 100 µl/CVs of DAPI (Sigma-Aldrich, D9542) (dilution 1:1000) were added for 10 minutes in the dark. The DAPI stains the nucleic acids.

The coverslips were rinsed in PBS/miliQ water/PBS three times each by. Then, they were dried with absorbent paper. After that, the coverslips were mount in slides using 15 µL of the Fluoromount-G® (SouthernBiotech, 0100-01) mounting medium.

Finally, images were taken using the SP8 LIGHTNING confocal microscope (Leica Microsystems) with a 63x objective. Excitation and emission wavelengths of the different fluorophores are showed in table 5.

Table 5. Excitation and emission wavelengths (nm) of the fluorophores used in the immunofluorescence.

	Λ excitation (nm)	**λ emission (nm)**	
Anti-Rabbit CF 647	651	670	Far red
DAPI	358	461	Blue
GFP	490	509	Green
LipidTOX	582	615	Red

3.7. Statistics analysis

To study the expression of ZNF423 in the mouse samples, a one-way ANOVA was performed, followed by Sidak's multiple comparisons test.

To evaluate the differences in expression according to the type of sample (control and overexpression or control and silencing) and according to the differentiation time, a "Two-way ANOVA" was performed, followed by the "Sidak's multiple comparisons test".

All analyses were performed with GraphPad software, presenting the data as mean ± standard deviation (SD). Differences were considered significant when: *$*P < 0.05$; **$P < 0.01$; ***$P < 0.001$*.

4. RESULTS AND DISCUSSION

4.1. Profiling ZNF423 mRNA expression in white adipose tissue of IRS2 KO mice exposed to different nutritional conditions

Our objective here was to study the ZNF423 mRNA profile in white adipose tissue of IRS2 KO mice exposed to different nutritional conditions. ZNF423 mRNA levels were measured in fed and fasting male and females IRS2 KO and control mice.

As shown in figure 3, mice underwent fasting exhibited higher levels of ZNF423 compared to mice that were fed, regardless of their gender. We observed a slight difference between males and females, with males generally showing a higher

expression profile of ZNF423 compared to females. In male white adipose tissue (WAT), a slight decrease in ZNF423 expression was observed in fasting conditions when comparing knockout (KO) mice to wild-type (WT) mice. Conversely, in females, the expression of ZNF423 increased with fasting in WT mice. Comparing fasting KO females to WT females, fasting appeared to promote a decrease in ZNF423 expression. We also checked the expression levels of IRS2 in WAT of these mice under the same nutritional conditions (supplementary figure S2). Under these conditions, our results show that ZNF423 follows the same expression pattern as IRS2 (supplementary figure S2). This could indicate us that ZNF423 could have a role downstream IRS2 in the insulin signalling pathway.

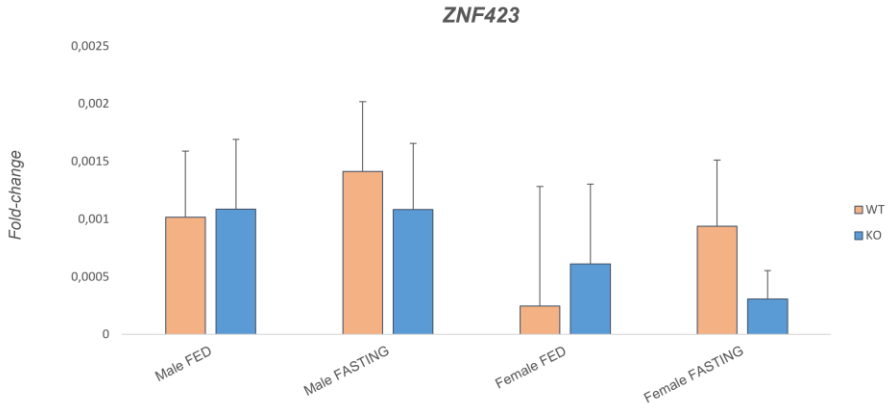

Figure 3. ZNF423 mRNA expression levels in WAT of WT and IRS2 KO fed and fasted mice. *ZNF423 mRNA expression levels (Fold-change) in fed and fasting male and females, IRS2 knock-out (KO) and wild-type (WT). Housekeeping genes: 18S, 36B4, PPIA, RPL19. Error bars indicate the SD. IRS2 WT and IRS2 KO [males fed (n = 9 and n = 10), males fasting (n = 4 and n = 8), female fed (n = 7 and n = 7), female fasting (n = 10 and n = 10)], respectively.* Statistically, no significant differences were found *(Two-way ANOVA with Sidak's multiple comparisons test).*

4.2. Morphological, mRNA and protein analysis of the 3T3-L1 cells overexpressing IRS2

3T3-L1 cells were infected with a lentivirus overexpressing IRS2. This cell line of preadipocytes was chosen because it is widely used in studies of adipogenesis and lipid metabolism (Kajimura et al., 2008; Reznikoff et al., 1973; Tang et al., 2004).

The response of ZNF423 to IRS2 overexpression condition in 3T3-L1 cells was studied at morphological, mRNA and protein level.

4.2.1. Morphological analysis of the 3T3-L1 cells overexpressing IRS2 during their differentiation process

Images of the adipocytes at different days throughout the differentiation process were taken, aiming to investigate potential morphological alterations resulting from IRS2 overexpression. It was observed (Figure 4) that between cells that did not overexpress

IRS2 and those that did overexpress it, there was no difference. Both showed the typical morphological transformations that preadipocytes undergo during differentiation. In the first few days, the cells showed a more stretched fibroblast-like shape: From day 5 they started to become spherical and accumulate lipid droplets, which increased in size as differentiation advanced (Grunfeld & Gorden, 1983).

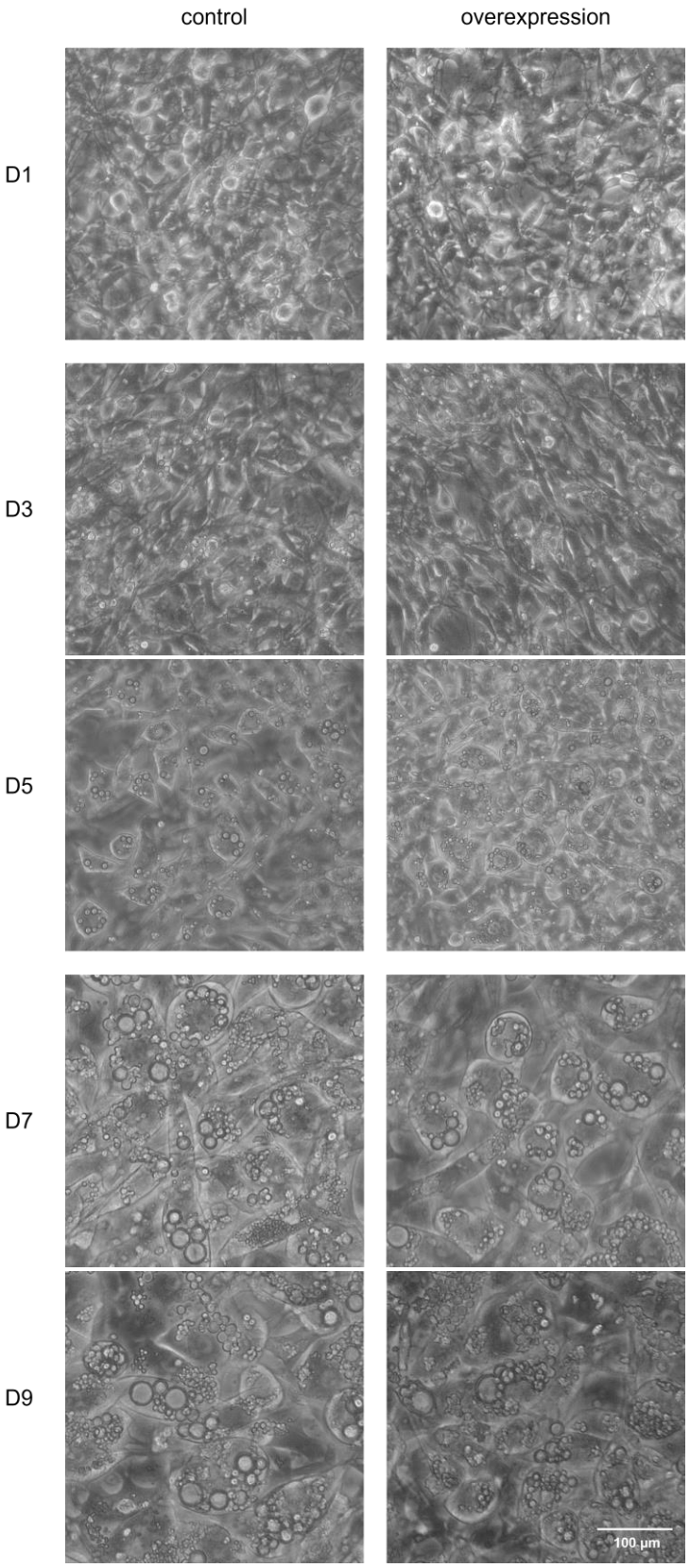

Figure 4. Morphological analysis of the 3T3-L1 cells overexpressing IRS2 during the differentiation process. *Images were taken during the differentiation process at different days (D1, 3, 5, 7 and 9) in 3T3-L1 cells overexpressing IRS2 and control cells. Scale bar: 100 µm.*

4.2.2. IRS2 and ZNF423 mRNA expression levels in 3T3-L1 overexpressing IRS2

IRS2 and ZNF423 mRNA levels during the differentiation were measured by RT-qPCR. In this experiment, 36B4, PPIA and RPL19 were used as housekeeping genes (table supplementary S1).

According to Figure 5, there seemed to be an overexpression of IRS2 in cells that were overexpressing IRS2 compared to control cells during the first two days of differentiation. However, from D5 onwards, the control cells exhibited higher IRS2 expression. Unfortunately, there was a technical issue during the cDNA synthesis process on day 3, which resulted in uninterpretable RT-qPCR results for that particular point.

Regarding the expression pattern of IRS2 during differentiation, a significant difference was observed between control cells and cells overexpressing IRS2 (with a p-value < 0,05) if the time variable was not considered. The main statistical difference was found when comparing control vs overexpression cells at day 7. Furthermore, IRS2 levels increased in the initial days and then decreased towards the later stages of differentiation (p-value < 0,001).

Similarly, ZNF423 followed a similar pattern. The mRNA levels increased during the early days of differentiation and decreased towards the later stages (p-value < 0,0001), with the exception of ZNF423 levels at day 0 when it exhibited higher expression than IRS2. Moreover, there are also significant differences between control and overexpression (p-value < 0,05) all along the differentiation days.

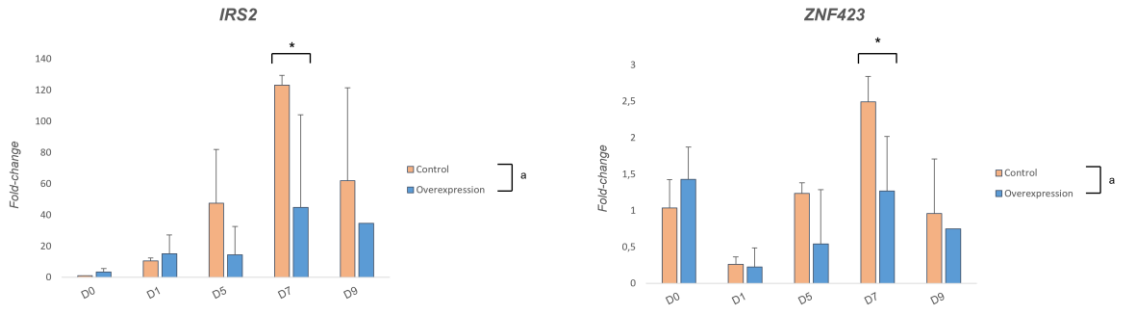

Figure 5. IRS2 and ZNF423 mRNA expression levels of the 3T3-L1 cells overexpressing IRS2 during the differentiation process. *mRNA expression levels (Fold-change) at different days (D0, 1, 5 ,7 and 9) in the 3T3-L1 cells overexpressing IRS2 and control cells. Housekeeping genes: 36B4, PPIA, RPL19. All the results were represented as the mean ± SD, n = 3 technical replicates. * P < 0.05; a = P < 0,05 (Two-way ANOVA with Sidak's multiple comparisons test).*

4.2.3. IRS2, ZNF423 and adipogenic protein expression levels in 3T3-L1 overexpressing IRS2

To investigate whether the observed mRNA expression pattern of IRS2 and ZNF423 could be translated to the protein level, a Western Blot analysis was conducted. PLIN1 and PPARγ1/2 were used as markers of adipogenesis, since they are proteins involved in this process. GAPDH was used as loading control to normalise the expression of the proteins of interest. PLIN1 expression was detected at D7. PLIN1 is a key protein found in adipocyte lipid droplets and plays an important role in regulating lipid storage and mobilisation in fat cells. This protein is expressed in the late stages of adipogenesis (Zhang et al., 2021). Also, it is expected that PPARγ increases during adipocyte differentiation, being considered as a key regulator of this process (Ghaben & Scherer, 2019). As Figure 6 shows, PPARγ started to be significantly expressed at D3 and expression of both isoforms increase with the differentiation process. PPARγ1 is ubiquitously expressed in many tissues and also in adipose tissue. However, PPARγ2 is specific to adipocytes. Since in our experiment we observed that PPARγ2 is being expressed, this indicates to us that the process of adipogenesis occurred as expected (Li et al., 2017),

In contrast to the observed mRNA expression pattern of IRS2, its protein expression does not follow the same trend. IRS2 protein expression is only detected at day D1 and D7. Moreover, although IRS2 is more highly expressed in the overexpressing cells at D1, there is not a significant difference compared to the control cells at D7.

There are several reasons that could explain why the mRNA and protein expression levels of IRS2 do not match. Firstly, the half-life and stability of both mRNA and protein can be affected by different post-transcriptional and translational mechanisms. In addition, techniques employed and experimental errors can also influence differences between mRNA and protein expression levels (Baldi & Long, 2001; Szallasi, 1999).

Insulin binds to its cellular receptors, activating a signalling cascade, of which IRS2 is part. In this experiment, the medium containing insulin is added at D0, 3 and 6. The cells were collected at D0, 1, 3, 5, 7 and 9. In our experiment we can observe that IRS2 protein expression is detected at D1 and 7, which correspond to the day after the medium has been changed. This could explain why IRS2 expression is only detected at D1 and D7 since the insulin contained in the medium could stimulate IRS2 protein expression.

With this same experiment we wanted to study how ZNF423 was expressed during differentiation. However, unfortunately we could not detect any band corresponding to ZNF423 molecular weight in our WB analysis. Some of the factors that may influence the detection of proteins in an immunoblot include problems with the antibody, such as low affinity or specificity towards the protein of interest. In addition, sample conditions or technical problems, such as protein concentration and protein transfer efficiency, can affect the detection. Other factors to consider include inadequate membrane blocking, incorrect antibody dilution, inadequate incubation conditions. It is also possible that the protein of interest is present at very low levels or absent in the sample (Mahmood & Yang, 2012). We were able to detect ZNF423 in the silencing experiment. Also, we could observe other proteins in this one. For that reason, it would have been adequate to consider the antibody dilution to achieve ZNF423 detection.

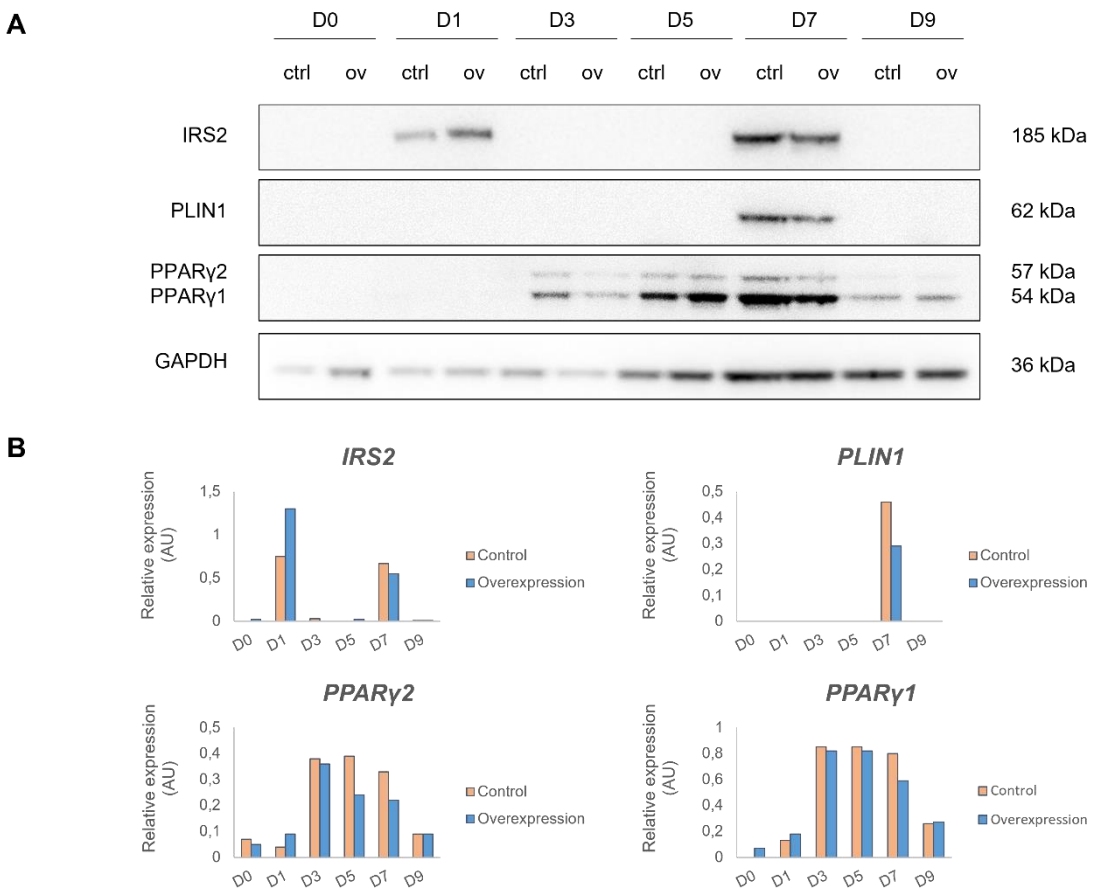

Figure 6. Protein expression levels of IRS2, PLIN1 and PPARγ in the 3T3-L1 cells overexpressing IRS2 and control cells during the differentiation process. *A) Bands obtained in the Western Blot analysis for IRS2 (gene of interest), PLIN1 and PPARγ (adipocytes differentiation positive control) and GAPDH (loading control) at different days (D0, D1, D3, D5, D7 and D9). B) Relative expression (Arbitrary Units) at protein level for IRS2, PLIN1, PPARγ1, PPARg2 and GAPDH at different days (D0, D1, D3, D5, D7 and D9)*

It should be noted that we did not detect an overexpression of IRS2 in the overexpression samples. This discrepancy could be attributed to several factors. Firstly, since the cells infected with the lentivirus cannot be easily identified or selected, it is possible that they were lost during the process of passaging and seeding the cells. Moreover, the experiment was performed with a n=1. To address these concerns and to confirm or rule out the initial results, it would be advisable to repeat the experiment. This would help to ensure the reliability and validity of the findings.

4.3. Morphological, mRNA and protein analysis of the 3T3-L1 cells silenced for IRS2

3T3-L1 cells were infected with a lentivirus carrying a siRNA for the silencing of IRS2. Then they were differentiated to mature adipocytes. During this differentiation process, cells were collected at different days in order to study mRNA and protein expression levels of the genes of interest. Cells growing on coverslips were also fixed with PFA 4% to study its morphological changes.

4.3.1. Morphological analysis of 3T3-L1 cells carrying IRS2 silencing during the differentiation process

Images of the adipocytes at different days of differentiation were taken. The goal here was to investigate potential morphological alterations due to IRS2 silencing. It was found (Figure 8) that there were no morphological differences between IRS2 silenced cells vs controls. As the overexpression experiment, both exhibit the normal morphological alterations that occur during adipocyte differentiation. Initially, the cells displayed a stretched, fibroblast-like shape. From day 5, they gradually transitioned into a rounder form and began to form lipid droplets, which get bigger as differentiation goes along.

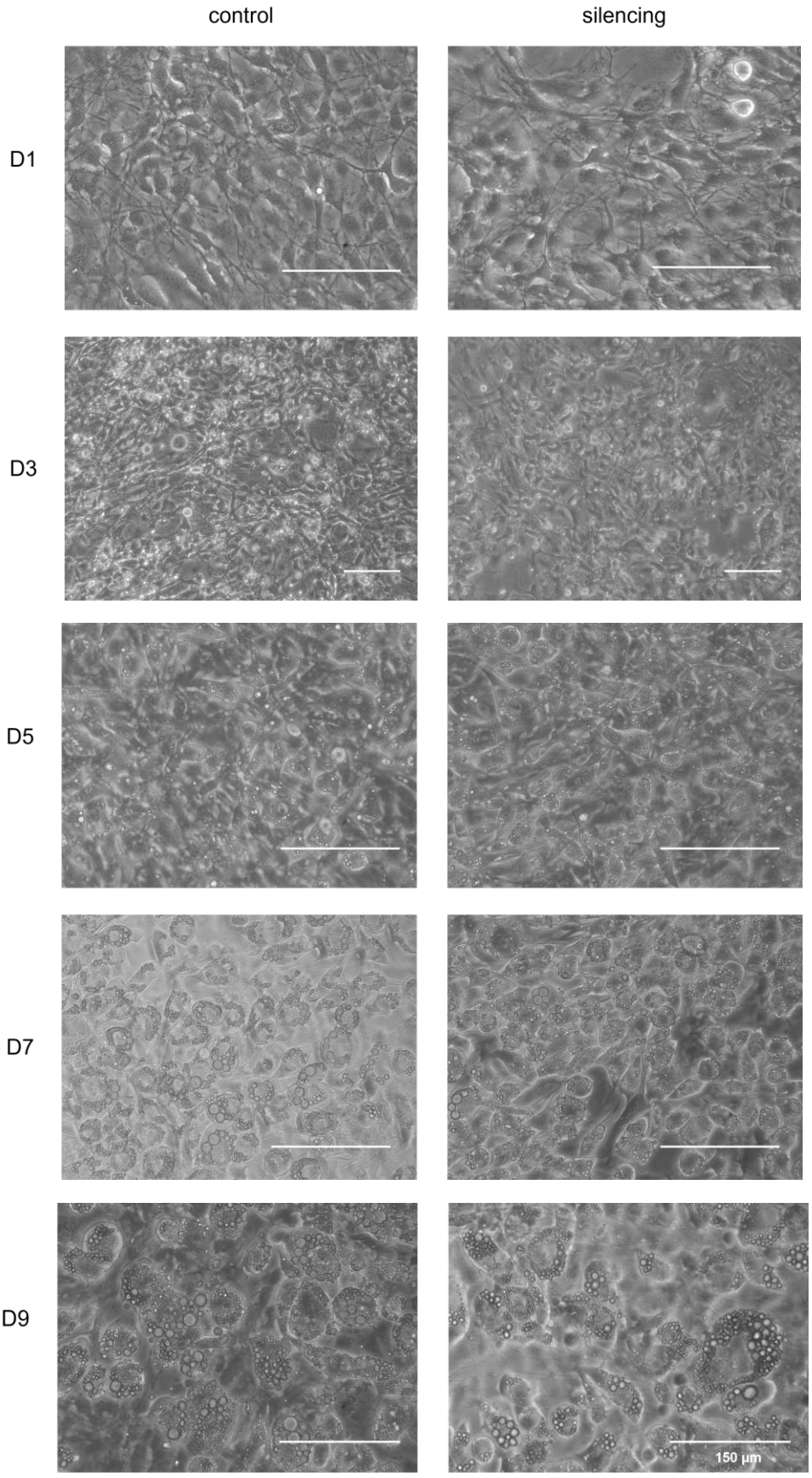

Figure 7. Morphological analysis of the 3T3-L1 carrying IRS2 silencing during the differentiation process. *Images during the differentiation process at different days (D1, 3, 5, 7 and 9) in 3T3-L1 cells silencing IRS2 and control cells. Scale bar: 150 µm.*

4.3.2. IRS2 and ZNF423 mRNA expression levels in 3T3-L1 silencing IRS2

As in the overexpressing experiment, IRS2 and ZNF423 mRNA levels during the differentiation were measured by RT-qPCR. In this experiment, 18S and 36B4 were used as housekeeping genes (table supplementary S1).

According to Figure 8, significant differences were observed in both IRS2 and ZNF423 expression profiles when comparing expression levels between days of differentiation (IRS2: p-value < 0.01; ZNF423: p-value < 0.05). However, no significant differences were observed between control and silencing IRS2 samples. It seems that the infection with lentivirus did not actually silence IRS2. One possible explanation could be that the silencing efficiency of the method used was not enough to knockdown IRS2 (Gavrilov & Saltzman, 2012).

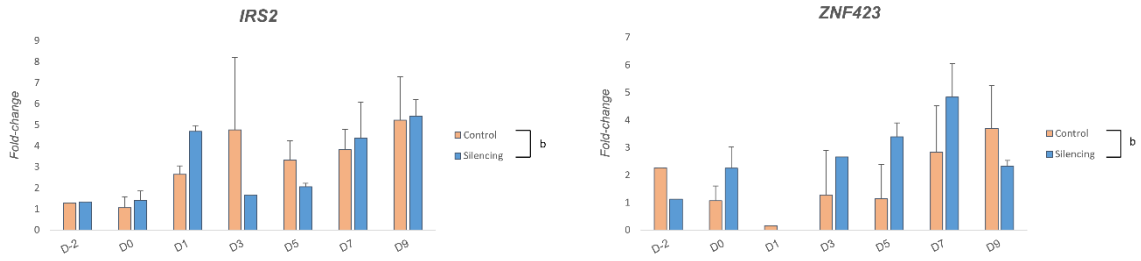

Figure 8. IRS2 and ZNF423 mRNA expression levels of the 3T3-L1 cells silencing IRS2 during the differentiation process. *mRNA expression levels (Fold-change) at different days (D-2, D0, D1, D3, D5, D7 and D9) in the 3T3-L1 cells silencing IRS2 and control cells. Housekeepigng genes: 18S and 36B4. Housekeeping genes: 36B4, PPIA, RPL19. All the results were represented as the mean ± SD, n = 3 technical replicates (no bar error: n = 1). b = no significant differences (Two-way ANOVA with Sidak's multiple comparisons test).*

4.3.3. Protein expression levels of IRS2 and ZNF423 in IRS2 silenced 3T3-L1 differentiating adipocytes

Western blot analysis was performed in order to study the protein expression levels of IRS2 and ZNF423 in the cells silenced for IRS2 vs control. In addition, to validate that the cells had integrated the IRS2-silencing lentivirus we checked the expression of GFP, since the lentiviral vector contains a GFP reporter gene to allow integration confirmation. In this case, as shown in the figure 9, the D5 control sample did not express as much GFP as the IRS2 silenced cells. It appears that there was an error in selecting the D5 sample for analysis. It was performed on the population of cells expressing low levels of GFP protein. On the other hand, GAPDH was used as loading control.

In the case of ZNF423, there were no notable differences observed between the control and IRS2-silenced cells, except for day 0, where a significantly higher amount of protein was detected in the IRS2-silenced cells. ZNF423 levels remained relatively stable throughout the differentiation process. Comparing the two experiments, IRS2 is not expressed during the same days of differentiation. In the previous experiment, we detected IRS2 at D1 and D7, while in this case it is only observed at D5. However, in both experiments, it was observed that on these particular days, both the treated and control cells expressed the IRS2 protein. Although the differentiation protocol is

standardised, there may have been experimental variations that led to these differences between the two experiments.

Like the overexpression study, this experiment was performed only once, so further experiments should be performed to confirm the results we obtained are reproducible.

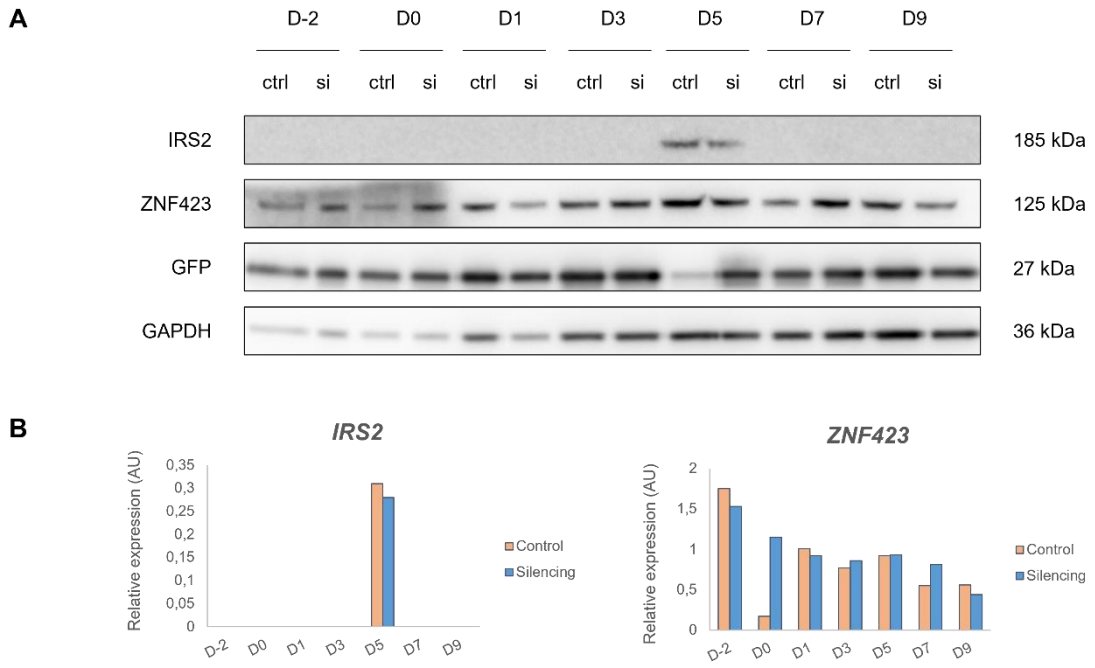

Figure 9. Protein expression levels of IRS2, ZNF423 and GFP in the 3T3-L1 cells silencing IRS2 and control cells during the differentiation process. *A) Bands obtained in the Western Blot analysis for IRS2 and ZNF423 (genes of interest), GFP (lentivirus infection positive control) and GAPDH (loading control) at different days (D-2, D0, D1, D3, D5, D7 and D9). B) Relative expression (Arbitrary Units) at protein level for IRS2 and ZNF423 at days -2, 0, 1, 3, 5, 7, 9.*

4.3.4. Immunofluorescence analysis of IRS2 knockdown 3T3-L1 cells during differentiation

Here our objective was to analyse in depth the possible adipocyte morphological changes due to IRS2 silencing. LipidTOX was used to stain lipid droplets since it binds to neutral lipids contained in them. DAPI was used to stain the nuclei as it is a cell-permeable fluorescent probe that binds to the minor groove of DNA, forming a stable complex that emits fluorescence. PLIN1 expression was also investigated by using a secondary antibody conjugated to CF™ 647, a cyanine-based superior far-red dye. Since the lentivirus used to silence IRS2 expressed GFP, its fluorescence could also be detected (Figure 10).

The images obtained (Figure 11) showed how lipid droplets increased in size as the differentiation process advanced. However, we did not observe any difference between control and IRS2-silenced cells. On the other hand, images also show that, as expected for a normal differentiation, PLIN1 was more expressed in the late stages of differentiation, (Shao et al., 2021).

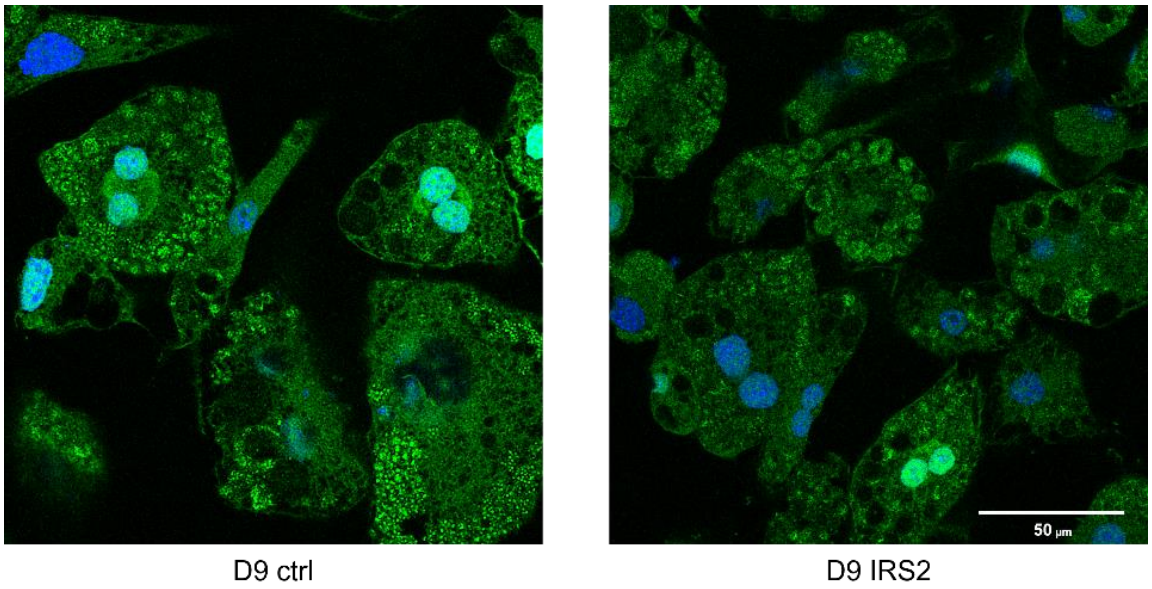

Figure 10. Morphological analysis by immunofluorescence of the 3T3-L1 cells carrying IRS2 silencing at day 9 of the differentiation. *Images of GFP (green) and nucleus (cyan) staining after the differentiation.*

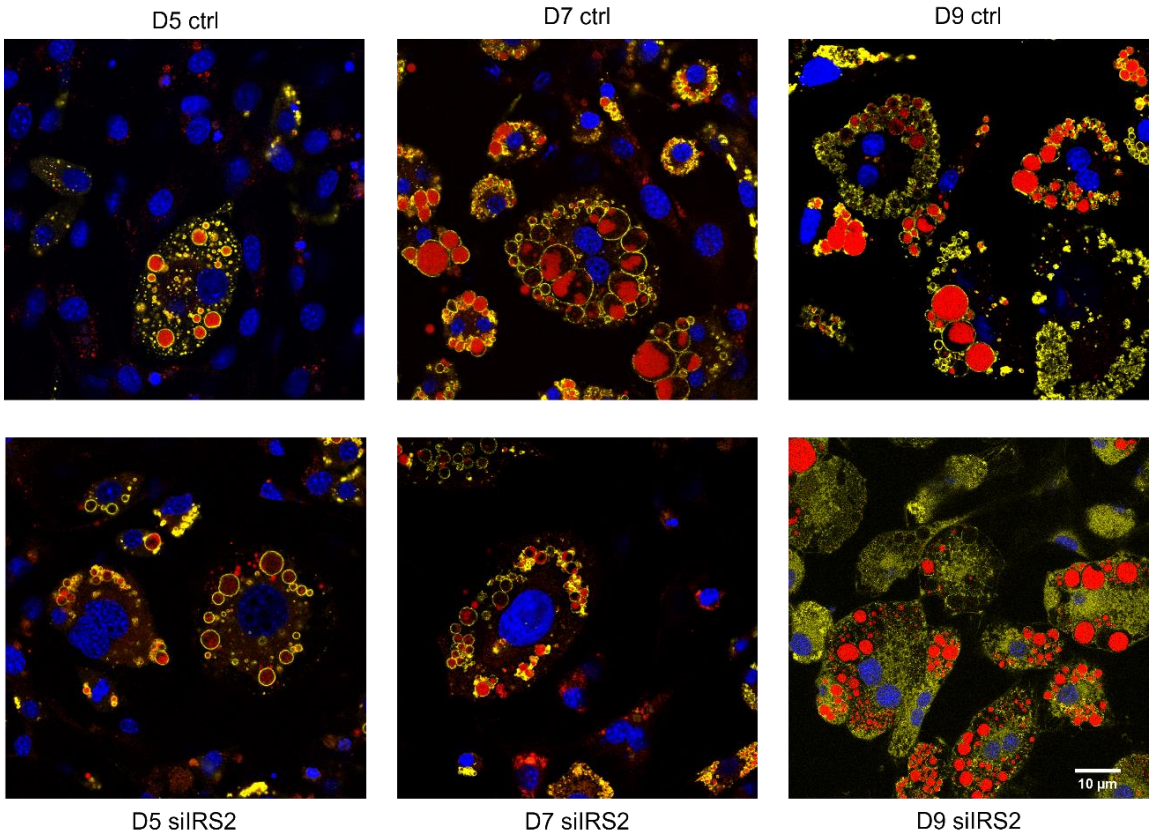

Figure 11. Morphological analysis by immunofluorescence of the 3T3-L1 cells carrying IRS2 silencing during the differentiation process. *Images of lipid, nuclei and PLIN1 staining after the differentiation. Lipids are shown in red, the nucleus in blue and PLIN1 in yellow.*

5. CONCLUSIONS

1. mRNA expression profile analysis of white adipose tissue of IRS2 KO mice under different nutritional conditions showed that ZNF423 is more expressed in males than females. IRS2 KO fed mice expressed more ZNF423 than fasted mice. Both IRS2 and ZNF423 seemed to follow the same expression pattern.

2. Morphological analysis in both the overexpression and silencing experiments showed that the adipocytes underwent the typical morphological changes expected during adipocyte differentiation. The cells have a fibroblast-like shape in the first days and become spherical and accumulate lipid droplets in the later stages.

3. In the IRS2 overexpression experiment, IRS2 protein was expressed at D1 and D7, which could be due to changes in the cell culture medium. In addition, it does not match the mRNA expression profile due to different reasons possible cellular regulatory mechanisms or experimental errors. ZNF423 could not be detected, which could be due to problems with the antibody, the sample or technical errors.

4. In the IRS2 silencing experiment, IRS2 protein was expressed at D5, while ZNF423 was expressed during all the differentiation. Also, the expression of GFP was detected what demonstrates that cells had integrated the lentivirus. Although mRNA levels do not follow a clear expression pattern, it seems that ZNF423 expression correlates to IRS2 levels. This could suggest that ZNF423 is downstream of IRS2 in the insulin signalling pathway.

5. Morphological analysis of IRS2 overexpressing and downregulating adipocyte by immunofluorescence showed how, as expected in a normal differentiation, lipid droplets grow in size and how PLIN1 expression increased as the differentiation process progressed.

6. BIBLIOGRAPHY

Ahima, R. S., & Flier, J. S. (2000). Adipose tissue as an endocrine organ. *Trends in Endocrinology and Metabolism*, *11*(8), 327–332. https://doi.org/10.1016/S1043-2760(00)00301-5

Ambele, M. A., Dhanraj, P., & Giles, R. (2020). *Adipogenesis A Complex Interplay of Multiple determinants and pathrways.pdf*.

Armani, A., Mammi, C., Marzolla, V., Calanchini, M., Antelmi, A., Rosano, G. M. C., Fabbri, A., & Caprio, M. (2010). Cellular models for understanding adipogenesis, adipose dysfunction, and obesity. *Journal of Cellular Biochemistry*, *110*(3), 564–572. https://doi.org/10.1002/jcb.22598

Baldi, P., & Long, A. D. (2001). *A Bayesian framework for the analysis of microarray expression data : regularized t -test and statistical inferences of gene changes*. *17*(6), 509–519.

Barrett, P., Mercer, J. G., & Morgan, P. J. (2016). Preclinical models for obesity research. *DMM Disease Models and Mechanisms*, *9*(11), 1245–1255. https://doi.org/10.1242/dmm.026443

Burks, D. J., & White, M. F. (2001). IRS proteins and beta-cell function. *Diabetes*, *50*(suppl_1), S140. https://doi.org/10.2337/diabetes.50.2007.s140

Carobbio, S., Rosen, B., & Vidal-Puig, A. (2013). Adipogenesis: New insights into brown adipose tissue differentiation. *Journal of Molecular Endocrinology*, *51*(3). https://doi.org/10.1530/JME-13-0158

Chaible, L. M., Kinoshita, D., Corat, M. A. F., & Dagli, M. L. Z. (2017). Genetically Modified Animal Models. In P. M. Conn (Ed.), *Animal Models for the Study of Human Disease* (Second, pp. 703–726). https://doi.org/10.1016/B978-0-12-809468-6/00027-9

Chooi, Y. C., Ding, C., & Magkos, F. (2019). The epidemiology of obesity. *Metabolism: Clinical and Experimental*, *92*, 6–10. https://doi.org/10.1016/j.metabol.2018.09.005

Clavijo, M. A., Camargo, D. G., & Alegría, C. G. (2007). in Vitro Adipogenesis of 3T3-L1 Cells. *Revista Med*, *15*(2), 170–174.

Copps, K. D., & White, M. F. (2012). Regulation of insulin sensitivity by serine/threonine phosphorylation of insulin receptor substrate proteins IRS1 and IRS2. *Diabetologia*, *55*(10), 2565–2582. https://doi.org/10.1007/s00125-012-2644-8

Dang, T. N., Tiongco, R. P., Brown, L. M., Taylor, J. L., Lyons, J. M., Lau, F. H., & Floyd, Z. E. (2022). Expression of the preadipocyte marker ZFP423 is dysregulated between well-differentiated and dedifferentiated liposarcoma. *BMC Cancer*, *22*(1), 1–15. https://doi.org/10.1186/s12885-022-09379-6

Fischer-posovszky, P. (2008). *Human SGBS Cells – a Unique Tool for Studies of Human Fat Cell Biology*. 184–189. https://doi.org/10.1159/000145784

Gavrilov, K., & Saltzman, W. M. (2012). *Therapeutic siRna : Principles , challenges ,. 85*, 187–200.

Ghaben, A. L., & Scherer, P. E. (2019). Adipogenesis and metabolic health. *Nature Reviews Molecular Cell Biology*, *20*(4), 242–258. https://doi.org/10.1038/s41580-018-0093-z

Grunfeld, C., & Gorden, P. (1983). *Morphological Changes Of The 3T3-L1 Fibroblast Plasma Membrane Upon Differentiation To The Adipocyte Form MORPHOLOGICAL CHANGES OF THE 3T3-L1 FIBROBLAST PLASMA MEMBRANE UPON DIFFERENTIATION TO THE ADIPOCYTE FORM*. *June*. https://doi.org/10.1242/jcs.61.1.219

Gupta, R. K., Mepani, R. J., Kleiner, S., Lo, J. C., Khandekar, M. J., Cohen, P., Frontini, A., Bhowmick, D. C., Ye, L., Cinti, S., & Spiegelman, B. M. (2012). Zfp423 expression identifies committed preadipocytes and localizes to adipose endothelial and perivascular cells. *Cell Metabolism*, *15*(2), 230–239. https://doi.org/10.1016/j.cmet.2012.01.010

Hafidi, M. El, Buelna-Chontal, M., Sánchez-Muñoz, F., & Carbó, R. (2019). Adipogenesis: A necessary but harmful strategy. *International Journal of Molecular Sciences*, *20*(15), 1–27. https://doi.org/10.3390/ijms20153657

Halberg, N., Khan, T., Trujillo, M. E., Wernstedt-Asterholm, I., Attie, A. D., Sherwani, S., Wang, Z. V., Landskroner-Eiger, S., Dineen, S., Magalang, U. J., Brekken, R. A., & Scherer, P. E. (2009). Hypoxia-Inducible Factor 1α Induces Fibrosis and Insulin Resistance in White Adipose Tissue. *Molecular and Cellular Biology*, *29*(16), 4467–4483. https://doi.org/10.1128/mcb.00192-09

Ikeda, K., Maretich, P., & Kajimura, S. (2018). The Common and Distinct Features of Brown and Beige Adipocytes. *Trends in Endocrinology and Metabolism*, *29*(3), 191–200. https://doi.org/10.1016/j.tem.2018.01.001

Jakab, J., Miškić, B., Mikšić, Š., Juranić, B., Ćosić, V., Schwarz, D., & Včev, A. (2021). Adipogenesis as a potential anti-obesity target: A review of pharmacological treatment and natural products. *Diabetes, Metabolic Syndrome and Obesity*, *14*, 67–83. https://doi.org/10.2147/DMSO.S281186

Kajimura, S., Seale, P., Tomaru, T., Erdjument-bromage, H., Cooper, M. P., Ruas, J. L., Chin, S., Tempst, P., Lazar, M. A., & Spiegelman, B. M. (2008). *Regulation of the brown and white fat gene programs through a PRDM16 / CtBP transcriptional complex*. 1397–1409. https://doi.org/10.1101/gad.1666108.in

Kleinert, M., Clemmensen, C., Hofmann, S. M., Moore, M. C., Renner, S., Woods, S. C., Huypens, P., Beckers, J., De Angelis, M. H., Schürmann, A., Bakhti, M., Klingenspor, M., Heiman, M., Cherrington, A. D., Ristow, M., Lickert, H., Wolf, E., Havel, P. J., Müller, T. D., & Tschöp, M. H. (2018). Animal models of obesity and diabetes mellitus. *Nature Reviews Endocrinology*, *14*(3), 140–162. https://doi.org/10.1038/nrendo.2017.161

Lee, J.-E., Schmidt, H., Lai, B., & Ge, K. (2019). Transcriptional and Epigenomic Regulation of Adipogenesis. *Molecular and Cellular Biology*, *39*(11). https://doi.org/10.1128/mcb.00601-18

Lefterova, M. I., & Lazar, M. A. (2009). New developments in adipogenesis. *Trends in Endocrinology and Metabolism*, *20*(3), 107–114. https://doi.org/10.1016/j.tem.2008.11.005

Li, D., Zhang, F., Zhang, X., Xue, C., Namwanje, M., Fan, L., Reilly, M. P., Hu, F., Qiang, L., Biology, C., Berrie, N., Syndrome, M., & Hospital, S. X. (2017). *Distinct Functions of PPARg Isoforms in Regulating Adipocyte Plasticity*. 1–15. https://doi.org/10.1016/j.bbrc.2016.10.152.Distinct

Livak, K. J., & Schmittgen, T. D. (2001). Analysis of relative gene expression data using real-time quantitative PCR and the 2-ΔΔCT method. *Methods*, *25*(4), 402–408. https://doi.org/10.1006/meth.2001.1262

Lizcano, F. (2019). The beige adipocyte as a therapy for metabolic diseases. *International Journal of Molecular Sciences*, *20*(20). https://doi.org/10.3390/ijms20205058

Lizcano, J. M., & Alessi, D. R. (2002). The insulin signalling pathway. *Current Biology*, *12*(7), 236–238. https://doi.org/10.1016/S0960-9822(02)00777-7

Longo, M., Zatterale, F., Naderi, J., Parrillo, L., Formisano, P., Raciti, G. A., Beguinot, F., & Miele, C. (2019). Adipose tissue dysfunction as determinant of obesity-associated metabolic complications. *International Journal of Molecular Sciences*, *20*(9). https://doi.org/10.3390/ijms20092358

Lutz, T. A., & Woods, S. C. (2012). Overview of animal models of obesity. *Current Protocols in Pharmacology*, *SUPPL.58*, 1–18. https://doi.org/10.1002/0471141755.ph0561s58

Mahmood, T., & Yang, P. (2012). *Western Blot : Technique , Theory , and Trouble Shooting*. *4*(9). https://doi.org/10.4103/1947-2714.100998

Manohar, S., Yu, Q., Gygi, S. P., & King, R. W. (2020). The insulin receptor adaptor IRS2 is an APC/C substrate that promotes cell cycle protein expression and a robust spindle assembly checkpoint. *Molecular & Cellular Proteomics*, *096238*(617), 1–35.

Miki, H., Yamauchi, T., Suzuki, R., Komeda, K., Tsuchida, A., Kubota, N., Terauchi, Y., Kamon, J., Kaburagi, Y., Matsui, J., Akanuma, Y., Nagai, R., Kimura, S., Tobe, K., & Kadowaki, T. (2001). Essential Role of Insulin Receptor Substrate 1 (IRS-1) and IRS-2 in Adipocyte Differentiation. *Molecular and Cellular Biology*, *21*(7), 2521–2532. https://doi.org/10.1128/mcb.21.7.2521-2532.2001

Muthu, M. L., & Reinhardt, D. P. (2020). Fibrillin-1 and fibrillin-1-derived asprosin in adipose tissue function and metabolic disorders. *Journal of Cell Communication and Signaling*, *14*(2), 159–173. https://doi.org/10.1007/s12079-020-00566-3

Myers, M. G., & White, M. F. (1996). Insulin signal transduction and the IRS proteins. *Annual Review of Pharmacology and Toxicology*, *36*(1), 615–658. https://doi.org/10.1146/annurev.pa.36.040196.003151

NIH. (2023). *ZNF423*. https://www.ncbi.nlm.nih.gov/gene/23090

Poulos, S. P., Dodson, M. V., & Hausman, G. J. (2010). Cell line models for differentiation: Preadipocytes and adipocytes. *Experimental Biology and Medicine*, *235*(10), 1185–1193. https://doi.org/10.1258/ebm.2010.010063

Reznikoff, C. A., Bertram, J. S., Brankow, D. W., & Heidelberger, C. (1973). *Quantitative and Qualitative Studies of Chemical Transformation of Cloned C3H Mouse Embryo Cells Sensitive to Postconfluence Inhibition of Cell Division1*. *December*, 3239–3249.

Rui, L. (2017). Brown and beige adipose tissues in health and disease. *Comprehensive Physiology*, *7*(4), 1281–1306. https://doi.org/10.1002/cphy.c170001

Ruiz-Ojeda, F. J., Rupérez, A. I., Gomez-Llorente, C., Gil, A., & Aguilera, C. M. (2016). Cell models and their application for studying adipogenic differentiation in relation to obesity: A review. *International Journal of Molecular Sciences*, *17*(7), 1–26. https://doi.org/10.3390/ijms17071040

Saely, C. H., Geiger, K., & Drexel, H. (2011). Brown versus white adipose tissue: A mini-review. *Gerontology*, *58*(1), 15–23. https://doi.org/10.1159/000321319

Sarjeant, K., & Stephens, J. M. (2012). *Adipogenesis*. 1–20.

Schelbert, K. B. (2009). Comorbidities of Obesity. *Primary Care - Clinics in Office Practice*, *36*(2), 271–285. https://doi.org/10.1016/j.pop.2009.01.009

Shao, M., Zhang, Q., Truong, A., Shan, B., Vishvanath, L., Li, L., Seale, P., & Gupta, R. K. (2021). ZFP423 controls EBF2 coactivator recruitment and PPARγ occupancy to determine the thermogenic plasticity of adipocytes. *Genes and Development*, *35*(21–22), 1461–1474. https://doi.org/10.1101/GAD.348780.121

Spalding, K. L., Arner, E., Westermark, P. O., Bernard, S., Buchholz, B. A., Bergmann, O., Blomqvist, L., Hoffstedt, J., Näslund, E., Britton, T., Concha, H., Hassan, M., Rydén, M., Frisén, J., & Arner, P. (2008). Dynamics of fat cell turnover in humans. *Nature*, *453*(7196), 783–787. https://doi.org/10.1038/nature06902

Szallasi, Z. (1999). *GENETIC NETWORK ANALYSIS IN LIGHT OF MASSIVELY PARALLEL BIOLOGICAL DATA ACQUISITION . 16*, 5–16.

Tang, Q., Otto, T. C., & Lane, M. D. (2004). *Commitment of C3H10T1 ¯2 pluripotent stem cells to the adipocyte lineage*. *4*(8), 1–5. https://doi.org/10.1073/pnas.0403100101

Taniguchi, C. M., Emanuelli, B., & Kahn, C. R. (2006). Critical nodes in signalling pathways: Insights into insulin action. *Nature Reviews Molecular Cell Biology*, *7*(2), 85–96. https://doi.org/10.1038/nrm1837

Thomson, J. A., Itskovitz-eldor, J., Shapiro, S. S., Waknitz, M. A., Swiergiel, J. J., Marshall, V. S., & Jones, J. M. (1998). *Embryonic Stem Cell Lines Derived from Human Blastocysts*. *282*(November), 1145–1148.

Vázquez-Vela, M. E. F., Torres, N., & Tovar, A. R. (2008). White Adipose Tissue as Endocrine Organ and Its Role in Obesity. *Archives of Medical Research*, *39*(8), 715–728. https://doi.org/10.1016/j.arcmed.2008.09.005

Virtue, S., & Vidal-Puig, A. (2010). Adipose tissue expandability, lipotoxicity and the Metabolic Syndrome - An allostatic perspective. *Biochimica et Biophysica Acta - Molecular and Cell Biology of Lipids*, *1801*(3), 338–349. https://doi.org/10.1016/j.bbalip.2009.12.006

Withers, D. J., Gutierrez, J. S., Towery, H., Burks, D. J., Ren, J. M., Previs, S., Zhang, Y., Bernal, D., Pons, S., Shulman, G. I., Bonner-Weir, S., & White, M. F. (1998). Disruption of IRS-2 causes type 2 diabetes in mice. *Nature*, *391*(6670), 900–904. https://doi.org/10.1038/36116

Wronska, A., & Kmiec, Z. (2012). Structural and biochemical characteristics of various white adipose tissue depots. *Acta Physiologica*, *205*(2), 194–208. https://doi.org/10.1111/j.1748-1716.2012.02409.x

Zhang, K., Chen, X., & Zhang, P. (2021). *Perilipin2 is an Earlier Marker Than Perilipin1 for Identifying Adipocyte Regeneration in Fat Grafts Animal Model for Fat Transplantation*. *41*(6), 646–652. https://doi.org/10.1093/asj/sjaa360

Zhang, K., Yang, X., Zhao, Q., Li, Z., Fu, F., Zhang, H., Zheng, M., & Zhang, S. (2020). *Review Article Molecular Mechanism of Stem Cell Differentiation into Adipocytes and Adipocyte Differentiation of Malignant Tumor*. *2020*.

7. ANNEX

Supplementary Table S1. List of primers used in the RT-qPCR. *F, forward primer; R, reverse primer.*

Gene	Sequence
18S	F: CGGCTACCACATCCAAGGAA
	R: GTCGGAATTACCGCGGCT
36B4	F: TCTCCAGAGGCACCATTGAAA
	R: CTCGCTGGCTCCCACCTT
IRS2	F: TTTGCCCACAATTCCAAGCG
	R: TGCTGCCTTCACTGCTTTTC
PPIA	F: AGCATACAGGTCCTGGCATC
	R: TTCACCTCCCAAAGACCAC
RPL19	F: GGTGACCTGGATGAGAAGGA
	R: TTCAGCTTGTGGATGTGCTC
ZNF423	F: CGCGATCGGTGAAAGTTGAAGAG
	R: GGTCTGCCAGAGACTCGAAG

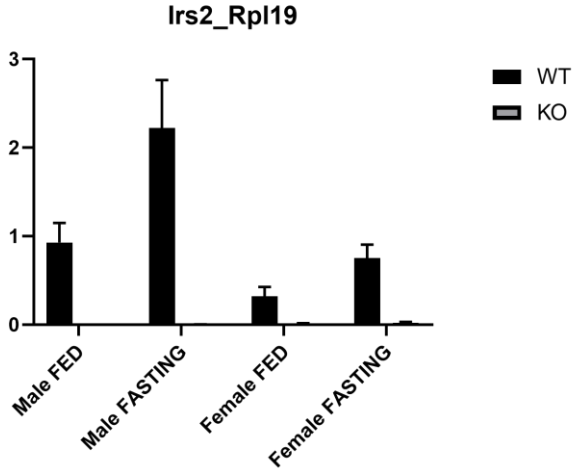

Supplementary Figure S2. IRS2 mRNA expression levels in mice. *IRS2 mRNA expression levels (Fold-change) in fed and fasting male and females, IRS2 knock-out (KO) and wild-type (WT). Rpl19 gene was used as housekeeping.*